iScience

Article

Circadian synchronization differentially modifies cytokine-mediated transcriptomic remodeling and cell death in INS-1 cells and mouse islets

Graphical abstract

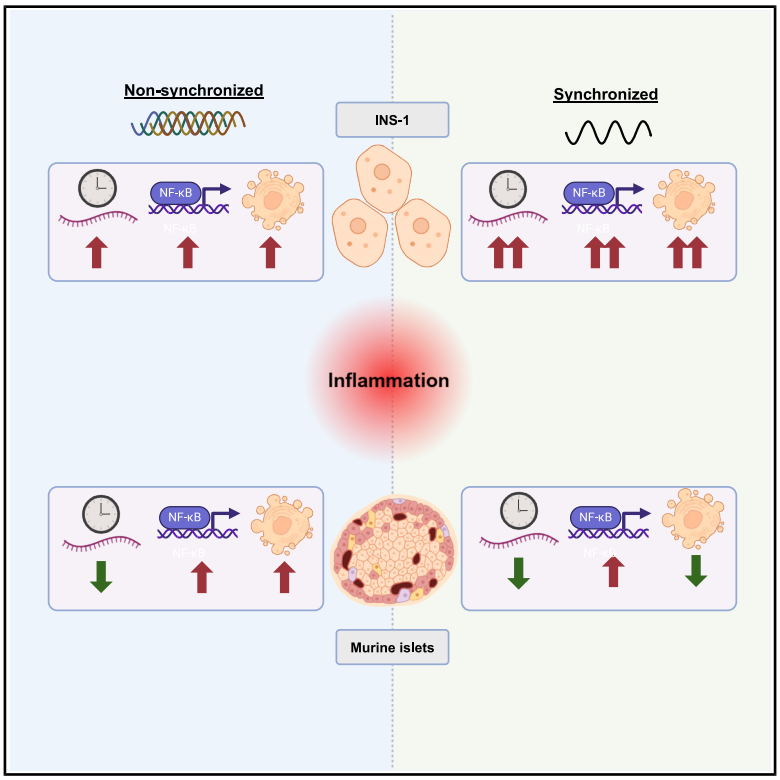

Authors

Phillip Alexander Keller Andersen, Rasmus H. Reeh, Isabel Sanders, ..., Anniek Frederike Lubberding, Charna Dibner, Thomas Mandrup-Poulsen

Correspondence

phillip.andersen@sund.ku.dk

In brief

Cell biology; Transcriptomics

Highlights

- Synchronization of β-cells differentially modifies cytokine-mediated outcomes
- Increased cell death, core clock expression, and NF-κB activity in INS-1 cells
- Reduced cell death, unaltered clock expression, and NF-κB activity in murine islets
- Differential effects depend on NF-κB involvement

Andersen et al., 2025, iScience *28*, 112431
May 16, 2025
https://doi.org/10.1016/j.isci.2025.112431

CellPress

iScience

CellPress
OPEN ACCESS

Article

Circadian synchronization differentially modifies cytokine-mediated transcriptomic remodeling and cell death in INS-1 cells and mouse islets

Phillip Alexander Keller Andersen,[1,7,*] Rasmus H. Reeh,[1] Isabel Sanders,[1,6] Emilie Bender Overlund,[1,6] Georgia Katsioudi,[2,3,4,5] Cecilia Jiménez-Sánchez,[2,3,4,5] Emil Zeng Skovhøj,[1] Anniek Frederike Lubberding,[1] Charna Dibner,[2,3,4,5] and Thomas Mandrup-Poulsen[1]

[1]Department of Biomedical Sciences, Faculty of Health and Medical Sciences, University of Copenhagen, 2200 Copenhagen N, Denmark
[2]Department of Surgery, Division of Thoracic and Endocrine Surgery, University Hospitals of Geneva, 1211 Geneva, Switzerland
[3]Department of Cell Physiology and Metabolism, Faculty of Medicine, University of Geneva, 1211 Geneva, Switzerland
[4]Diabetes Center, Faculty of Medicine, University of Geneva, 1211 Geneva, Switzerland
[5]Institute of Genetics and Genomics of Geneva (iGE3), 1211 Geneva, Switzerland
[6]These authors contributed equally
[7]Lead contact
*Correspondence: phillip.andersen@sund.ku.dk
https://doi.org/10.1016/j.isci.2025.112431

SUMMARY

Perturbation of the β-cell circadian clock causes oxidative stress and secretory failure, and proinflammatory cytokines disrupt the β-cell core clock. We hypothesized that cytokine-mediated clock perturbation in β-cells depends on circadian synchronization status. Cytokine-mediated core clock mRNA expression in non-synchronized insulin-producing INS-1 cells were potentiated upon synchronization, which were differentially translated into alterations in protein levels. Synchronization sensitized INS-1 cells to cytokine-mediated cytotoxicity, associated with potentiation of NF-κB activity. Inhibition of NF-κB abrogated cytokine-mediated clock gene-expression independent of synchronization status and reversed cytokine-mediated period lengthening. In contrast, in murine islets, cytokines generally reduced core clock mRNA expression independently of synchronization status or NF-κB activity. Synchronization prevented cytokine-mediated cytotoxicity, but not NF-κB activity to a degree comparable to that of KINK-1, while alterations in islet rhythmicity were unaffected by NF-κB inhibition. In conclusion, circadian synchronization differentially modifies cytokine-mediated transcriptomic remodeling and cell death in INS-1 cells and murine islets, depending on NF-κB involvement.

INTRODUCTION

The circadian system, highly conserved in evolution, enables light-sensitive organisms to anticipate, prepare for, and respond to regularly recurring physiological needs during a solar day.[1] To uphold circadian regulation at the systemic organismal level, almost all cells harbor intrinsic molecular clocks that operate via interlocked transcriptional-translational feedback loops.[1] Individual cellular molecular clocks are synchronized through multiple entrainment signals (*Zeitgebers*)[2] comprising light,[3] temperature,[4] nutrition,[5] and physical activity[6] that are integrated by the central clock in the suprachiasmatic nuclei to convey synchronizing neurohumoral signals to the peripheral oscillators.

Coordinated circadian oscillations are required for normal tissue functions, and circadian misalignment is a risk factor for common chronic diseases, e.g., neoplastic, cardio-metabolic, and psychiatric disorders.[7] Indeed, circadian disruption and misalignment confer β-cell dysfunction and insulin resistance,[8–11] while global or β-cell specific knock-out of core molecular clock activators results in β-cell secretory failure and diabetes.[12,13]

Inflammation is a common pathogenic factor in both type 1 and type 2 diabetes, and there is clinical proof-of-concept that proinflammatory cytokines contribute to β-cell failure in these diseases.[14–16] The molecular mechanisms underlying cytokine-mediated β-cell failure and destruction are incompletely understood but involve nuclear factor of kappa light polypeptide gene enhancer in B-cells (NF-κB) and mitogen-activated protein kinase (MAPK) activation, and nitroxidative, endoplasmic reticulum (ER) and mitochondrial stress that eventually trigger the intrinsic apoptosis program.[17,18]

NF-κB activation induces transcriptional reprogramming in β-cells, with extensive alterations of the expressional profiles of hundreds of both defensive and deleterious pathways. Many of the cytokine-induced β-cell transcriptomic changes ultimately causing secretory dysfunction and culminating in apoptosis are NO-, and thereby, NF-κB-dependent, in particular in rat β-cells.[18–21] Interestingly, in addition to its role in inflammation,

NF-κB signaling is required for a functional molecular clock,[22,23] indicating a context-dependent interplay between physiological and pathophysiological actions of NF-κB.

We and others[24,25] have recently found that proinflammatory cytokines reconfigure the expressional pattern of core clock genes, while also changing rhythmic parameters in islets harboring a period 2 promotor-driven Luciferase (*Per2:Luc*). We found that the proinflammatory cytokines interleukin-1β (IL-1β) and interferon-γ (IFN-γ) increased period length in both human and murine islets.[24] Further, we observed that brain and muscle arnt-like 1 (*Bmal1*), circadian locomotor output cycles kaput (*Clock*), nuclear receptor subfamily 1 group D member 1 (*Nr1d1* or *Rev-erbα*), *Per1, Per2* and cryptochrome 2 (*Cry2*) were upregulated, while *Cry1* was downregulated by these cytokines in the rat insulin-producing cell line INS-1. Interestingly, these apparently uncoordinated expressional changes were reversed by inhibiting inducible nitric oxide synthase (iNOS), histone deacetylase 3 (HDAC3), and the immune/intermediate proteasome. All these pathways are involved in inflammatory β-cell stress and regulated by NF-κB.[14,18,24,26] However, a direct demonstration that NF-κB signaling conveys proinflammatory stress-mediated clock gene alterations and period perturbation in β-cells is lacking. Furthermore, a main limitation in our previous study[24] was that gene expression levels were only determined in a non-synchronized model system without parallel documentation of β-cell viability under these conditions.

Cultured cells can be synchronized *in vitro* using different synchronization cues, such as serum shock, dexamethasone, forskolin pulsing, and many more.[27,28] We hypothesized that cytokine-mediated clock perturbation is NF-κB driven, as is cytokine-induced apoptosis, but these depend on the cellular synchronization status and the intensity of inflammatory stress. We demonstrate that circadian synchronization differentially modifies cytokine-mediated transcriptomic remodeling and cell death in insulin-producing cells and murine islets, depending on NF-κB involvement.

RESULTS

Proinflammatory cytokines introduce uncoordinated alterations in clock protein expression in INS-1 cells

As we have previously[24] investigated the effect of proinflammatory cytokines on core clock gene expression to assess the transcriptional response to inflammatory stress, we first wished to assess the protein levels of selected transcriptional repressors and activators. INS-1 cells were exposed to a combination of the proinflammatory cytokines IL-1β and IFN-γ for 8–36 h and harvested at 4-h intervals to allow for analysis of both cytokine-mediated and temporal effects. Protein levels of REV-ERBα, CRY2, BMAL1, and CLOCK were determined (Figure S1). These proteins were selected based on the effect sizes of the cytokine-induced transcriptional changes as reported in Andersen and Petrenko et al.[24] Cytokines significantly upregulated both CLOCK and REV-ERBα with an additional trend toward time dependency for CLOCK, which also showed a significant interaction between these in a two-way ANOVA.

Thus, IL-1β and IFN-γ upregulate the expression levels of a subset of the selected core clock proteins in INS-1 cells.

Synchronization potentiates the cytokine-mediated alterations in expression of core clock mRNAs and proteins, and of inducible proteasome transcripts in INS-1 cells

To investigate proinflammatory stress-mediated changes in core clock gene mRNA and protein levels in a more relevant circadian model, INS-1 cells harboring *Per2* promotor-driven luciferase (*Per2:Luc*), as a readout of integrated circadian rhythmicity, were synchronized *in vitro* by a 1-h 10 μM forskolin pulse, which is a known synchronization stimulus, preferentially used in the synchronization of β-cells.[13,29,30] Additionally, cells were subjected to medium change alone or direct administration of Luciferin (no media change) to control for cell handling. Forskolin induced an oscillatory rhythm distinct from that observed after cell handling (data not shown). The forskolin-induced rhythmic oscillations of circadian bioluminescence were concordant with endogenous core clock mRNA expression that showed anti-phasic rhythmic profiles between repressors and activators, also observed to a lesser extent at protein levels (Figures S2 and S3). In the following, "synchronized" will refer to cells exposed to a forskolin pulse, while "non-synchronized" will refer to cells not exposed to a forskolin pulse, even if they have some inherent rhythmicity.

Next, synchronized INS-1 cells were exposed to IL-1β and IFN-γ, and the expression levels of the selected clock gene mRNAs (Figure 1) and proteins (Figure 2) were investigated in a time-dependent manner. The cytokine-induced mRNA expression of *Rev-erbα*, *Per2,* and *Bmal1* was potentiated by synchronization (Figure 1), particularly notable at the peaks for *Bmal1* (a 48% increase) and *Rev-erbα* (a 46% increase). Cytokine-induced *Clock* expression was not changed by synchronization, while *Cry2* expression was not significantly affected.

Cytokine-induced REV-ERBα and CLOCK proteins were significantly increased by synchronization, with the time dependency also being affected (Figure 2). However, the activator protein BMAL1 and the repressor protein CRY2 remained unchanged after synchronization.

The transcriptional activity of the BMAL1-CLOCK heterodimer and the function of the clock repressors depend on proteasomal degradation.[1,31] Prompted by the observation that cytokine-mediated changes in clock gene mRNA expression in non-synchronized INS-1 cells were dependent on the inducible (ind)-proteasome,[24] we decided to investigate the effect of synchronization on ind-proteasome subunits in the absence and presence of cytokines. By analysis of a previously published dataset,[30] all three inducible subunits displayed circadian rhythmicity in synchronized mouse islets (Table S1). The resolution of our sampling and the 8-36-h time period studied with only one circadian cycle did not allow us to reproduce this finding by qPCR (Figure S4). However, synchronization significantly potentiated the cytokine-mediated alterations in *Psmb8* and *Psmb9*, but not *Psmb10* expression (Figure 3). Interestingly, bioinformatic analysis revealed that the selected core clock proteins harbor a higher number of ind-proteasomal, compared to standard proteasomal, target sites, indicating that these proteins can be targeted by the inducible proteasomes to a higher degree than by the standard proteasome (Table S2).

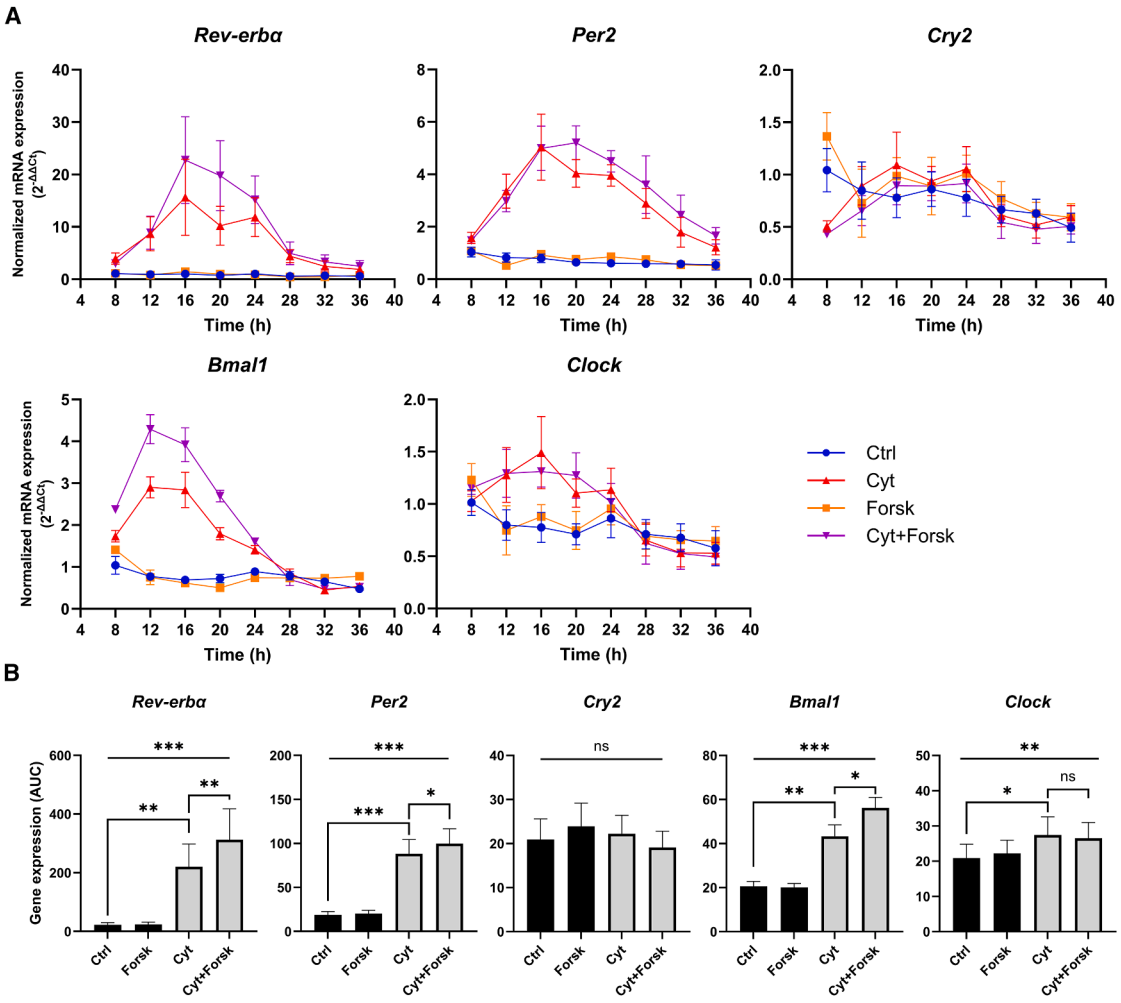

Figure 1. Synchronization potentiates the proinflammatory cytokine-mediated alterations in core clock gene expression

INS-1 cells were cultured in the presence (Cyt) or absence (Ctrl) of 150 pg/mL of mIL-1β and 0.1 ng/mL rIFN-γ. Additionally, cells were synchronized with a 1-h forskolin pulse in the absence (Forsk) or presence (Cyt+Forsk) of the same cytokine concentrations, as described in STAR Methods. Cells were exposed for between 8 and 36 h, with cell harvest at 4-h intervals. Normalized mRNA expression was calculated using *Hprt1* as a reference gene.

(A) Time-dependent normalized mRNA expression.

(B) AUC of the curves in (A). Data are presented as means ± SEM ($N = 4$). Statistics are repeated measurements ANOVA with Holm-Sidak's multiple comparisons test. Overall ANOVA p-value represented by symbols above the top line, while the brackets annotate comparisons. Significance levels are annotated as follows: ns = not significant, * = p-value <0.05, ** = p-value <0.01, and *** = p-value <0.001.

In summary, *in vitro* circadian synchronization of INS-1 cells potentiates the proinflammatory cytokine-mediated alterations in the expression of several core clock mRNAs along with REV-ERBα and CLOCK proteins, and ind-proteasome subunit mRNAs.

Cytokine-mediated core clock gene expression is NF-κB-dependent in INS-1 cells, with circadian synchronization potentiating NF-κB signaling

We anticipated that the cytokine-mediated alterations in clock gene mRNA expression were NF-κB dependent.[24] Therefore, we hypothesized that the potentiating effects of synchronization involved enhanced NF-κB signaling. To measure NF-κB activity, we investigated inducible nitric oxide (NO) synthase (*Inos*) expression, as its promotor contains several NF-κB *cis*-binding elements making *Inos* expression a highly sensitive NF-κB reporter. Further, NO, the product of iNOS, positively feedbacks on NF-κB transcriptional activity.[32] Indeed, forskolin-induced synchronization potentiated the expression of cytokine-mediated *Inos* expression (Figures 4A and 4B). As the expression of *Inos* in the investigated time frame was highest at 8 h, we wished to investigate an earlier time point. Synchronization potentiated *Inos* and *IκBα* expression, but not *Bmal1* at this early time point, in cytokine-exposed INS-1 cells (data not shown) indicating early NF-κB activation.

Since cytokine-induced *Inos* expression was enhanced in synchronized INS-1 cells, and since iNOS inhibition abrogated cytokine-mediated alterations in clock gene mRNA expression in non-synchronized INS-1 cells,[24] we next investigated the direct role of NF-κB in proinflammatory mediated clock gene alterations.

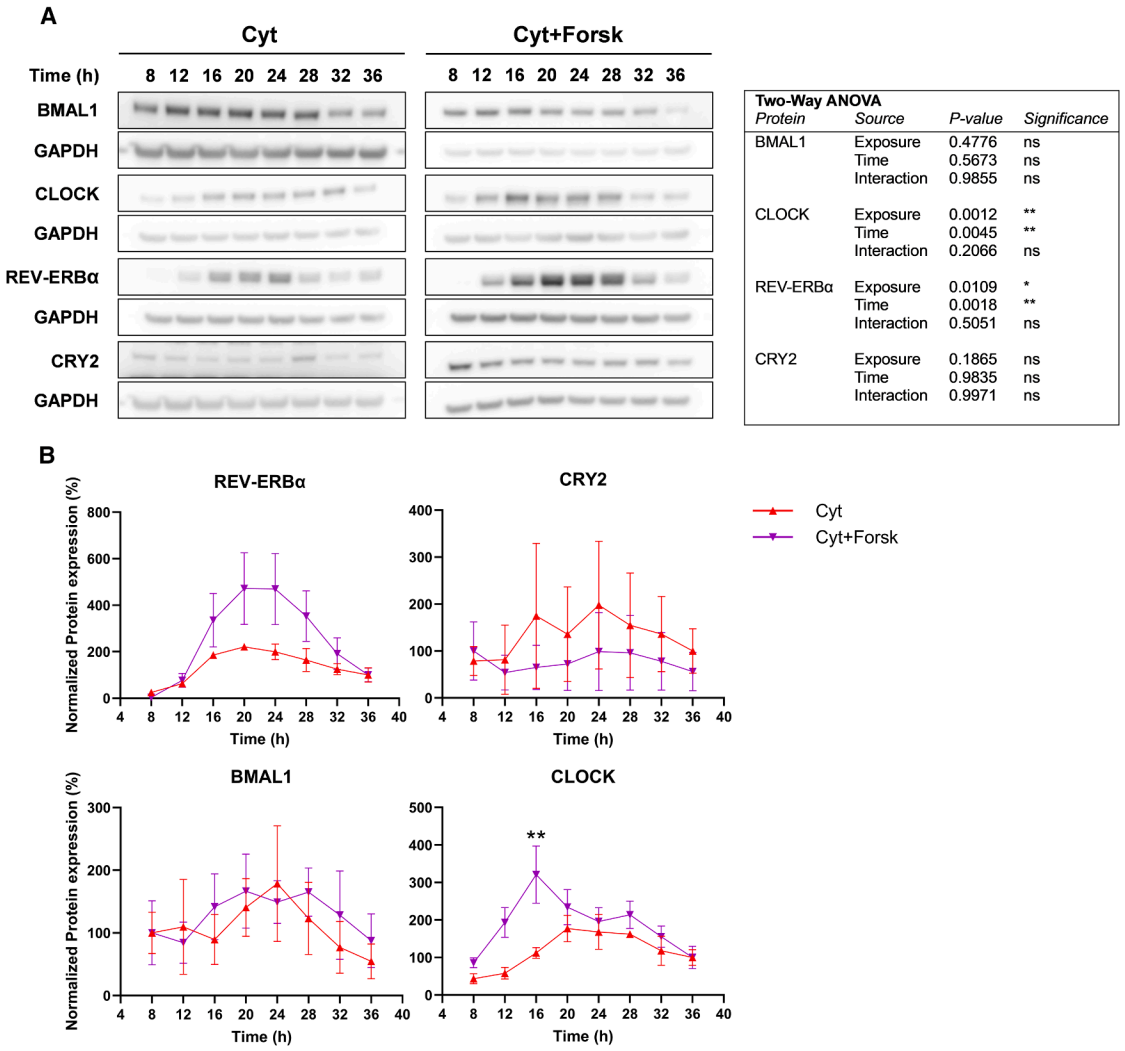

Two-Way ANOVA

Protein	*Source*	*P-value*	*Significance*
BMAL1	Exposure	0.4776	ns
	Time	0.5673	ns
	Interaction	0.9855	ns
CLOCK	Exposure	0.0012	**
	Time	0.0045	**
	Interaction	0.2066	ns
REV-ERBα	Exposure	0.0109	*
	Time	0.0018	**
	Interaction	0.5051	ns
CRY2	Exposure	0.1865	ns
	Time	0.9835	ns
	Interaction	0.9971	ns

Figure 2. Synchronization potentiates the proinflammatory cytokine-mediated increase in CLOCK and REV-ERBα expression

INS-1 cells were exposed as described in Figure 1, only using cytokine-exposed cells in a non-synchronized (Cyt) or synchronized (Cyt+Forsk) system.

(A) Samples were analyzed by SDS-PAGE and Western blotting with GAPDH as the internal loading control. Data of the different proteins of interest has been consolidated from multiple blots as illustrated by the boxed in bands, with protein of interest and loading control originating from the same blot in each case.

(B) Quantification and normalization of the protein expression levels. Data are presented as means ± SEM (N = 3–4, except for Cyt 12 h and Cyt+Forsk 8 h where *N* = 2 due to missing values). Statistics are two-way ANOVA with Holm-Sidak's corrected multiple comparisons tests. A summary of the statistical tests is presented in the table. Significance levels are annotated as follows: ns = not significant, * = *p*-value <0.05, and ** = *p*-value <0.01.

We targeted NF-κB by a small molecule, *IKKβ-selective Inhibitor of NF-κB* (IκB) *kinase* (IKK) inhibitor, KINK-1,[33] that by preventing phosphorylation of IκB blocks dissociation of IκB from p65 and thereby p65 nuclear translocation. One μM KINK-1, a dose selected from previous studies in our lab[34] and shown here to be non-toxic, rescued the cytokine-mediated loss of viability in non-synchronized cells as expected (data not shown). At 16 and 20 h of cytokine exposure, 1 μM KINK-1 also reduced the cytokine-mediated clock gene transcript alterations approximately to baseline levels in these cells (Figures 4C and S5). Unexpectedly, KINK-1 enhanced cytokine-induced *Psmb9* and *10* mRNA expression in non-synchronized cells, suggesting the existence of NF-κB dependent repressors of the expression of ind-proteasomal components (Figure S6A).

In synchronized cells, NF-κB inhibition differentially attenuated cytokine modulation of core clock transcripts (Figures 4C and S5) and ind-proteasomal subunit expression (Figure S6A), with the effect of KINK-1 in cytokine-exposed cells differing depending on the transcript in question. For *Rev-erbα*, *Per2*, and *Bmal1*, NF-κB inhibition reversed cytokine-mediated alterations at both 16 and 20 h, and at 16 h for *Clock* with the same trend (p = 0.0997) at 20 h (Figures 4C and S5). Synchronization reduced *Cry2* expression relative to the other conditions, and this inhibition was reversed by KINK-1 at 16 h.

KINK-1 exposure further increased cytokine-induced expression of *Psmb10* at both 16 and 20 h and of *Psmb9* at 20 h, with statistical trends at 16 h in both non-synchronized and synchronized cells (Figure S6A). *Psmb8* followed the pattern for *Psmb10*

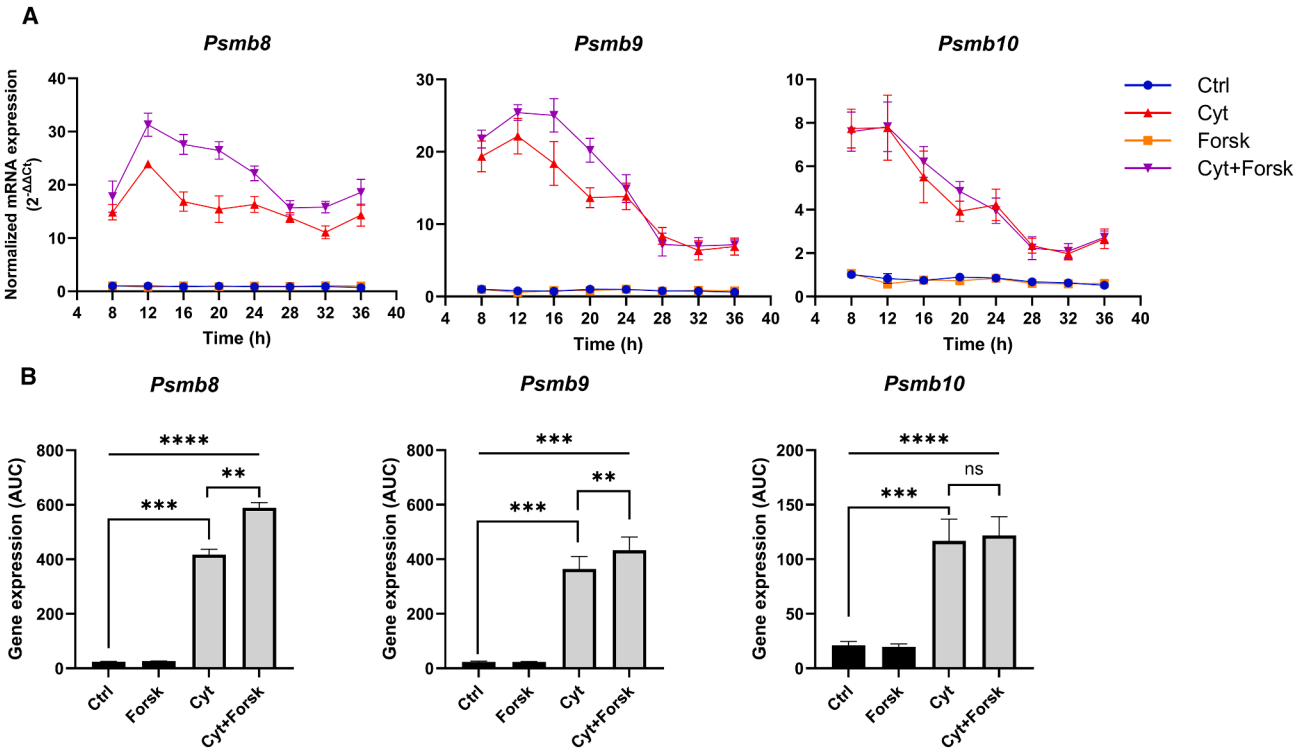

Figure 3. Synchronization potentiates the proinflammatory cytokine-mediated increase in ind-proteasome subunits

INS-1 cells were handled as described in Figure 1. Normalized mRNA expression was calculated using *Hprt1* as a reference gene.

(A) Time-dependent normalized mRNA expression of ind-proteasome subunits.

(B) AUC of the curves in (A). Data are presented as means ± SEM ($N = 4$). Statistics are repeated measurements ANOVA with Holm-Sidak's multiple comparisons test. Overall ANOVA p-value represented by symbols above the top line, while the brackets annotate comparisons. Significance levels are annotated as follows: ns = not significant, ** = p-value <0.01, *** = p-value <0.001, and **** = p-value <0.0001.

and -*9* regarding the potentiating effect of KINK-1 on cytokine-induced expression in non-synchronized cells, but with the opposite pattern in synchronized cells as indicated by the overall significant ANOVA. However, these differences were not significant in post-hoc t-tests.

To better appreciate the impact of KINK-1 on cytokine-mediated alterations of clock and proteasome mRNAs in synchronized vs. non-synchronized cells, the percentage change in expression caused by NF-κB inhibition during cytokine exposure was calculated, correcting for the baseline expression in non-cytokine exposed cells (Figure S6B). In general, the relative effect sizes of NF-κB inhibition on the expression of both clock and ind-proteasomal genes were attenuated in synchronized vs. non-synchronized cells (Figure S6B).

To summarize, NF-κB inhibition differentially attenuates cytokine-mediated alterations in core clock gene transcripts and ind-proteasomal subunit expression in INS-1 cells.

Cytokines reduce core clock mRNA expression in intact murine islets independently of synchronization status and NF-κB activity

After investigating the effects of synchronization in a β-cell line lacking paracrine relations to other endocrine pancreatic cells, we wished to examine the interplay between proinflammatory stress and circadian synchronization in murine islets with intact cellular biosociology. Non-synchronized or synchronized murine islets were exposed to IL-1β and IFN-γ for 12 h in the presence or absence of KINK-1 (Figure 5). Interestingly, and in contrast to the observations in INS-1 cells, proinflammatory cytokines generally reduced core clock mRNA expression of both activators and repressors in murine islets independently of synchronization status or NF-κB activity, suggesting different clock gene transcriptional responses to cytokines and underlying mechanisms in β-cells and intact islets.

Synchronization potentiates cytokine-induced β-cell endoplasmic reticulum stress and the intrinsic apoptotic pathway in INS-1 cells

NO is a key conveyor of cytokine-mediated ER stress, since NO inhibits the sarcoplasmic/endoplasmic reticulum Ca^{2+}-ATPase (SERCA) pump, causing ER Ca^{2+} depletion.[20] Therefore, we explored if ER stress markers were affected by synchronization of cytokine-exposed INS-1 cells. Both cytokine-induced *Bip* and *Atf4* expression and *Xbp (sXbp1)* splicing (Figure 6) were modestly potentiated by synchronization, with total and unspliced *Xbp1* showing a trend in the overall ANOVA (Figure S7).

The cytokine-induced ER stress response is believed to contribute to activation of the intrinsic (mitochondrial), but not

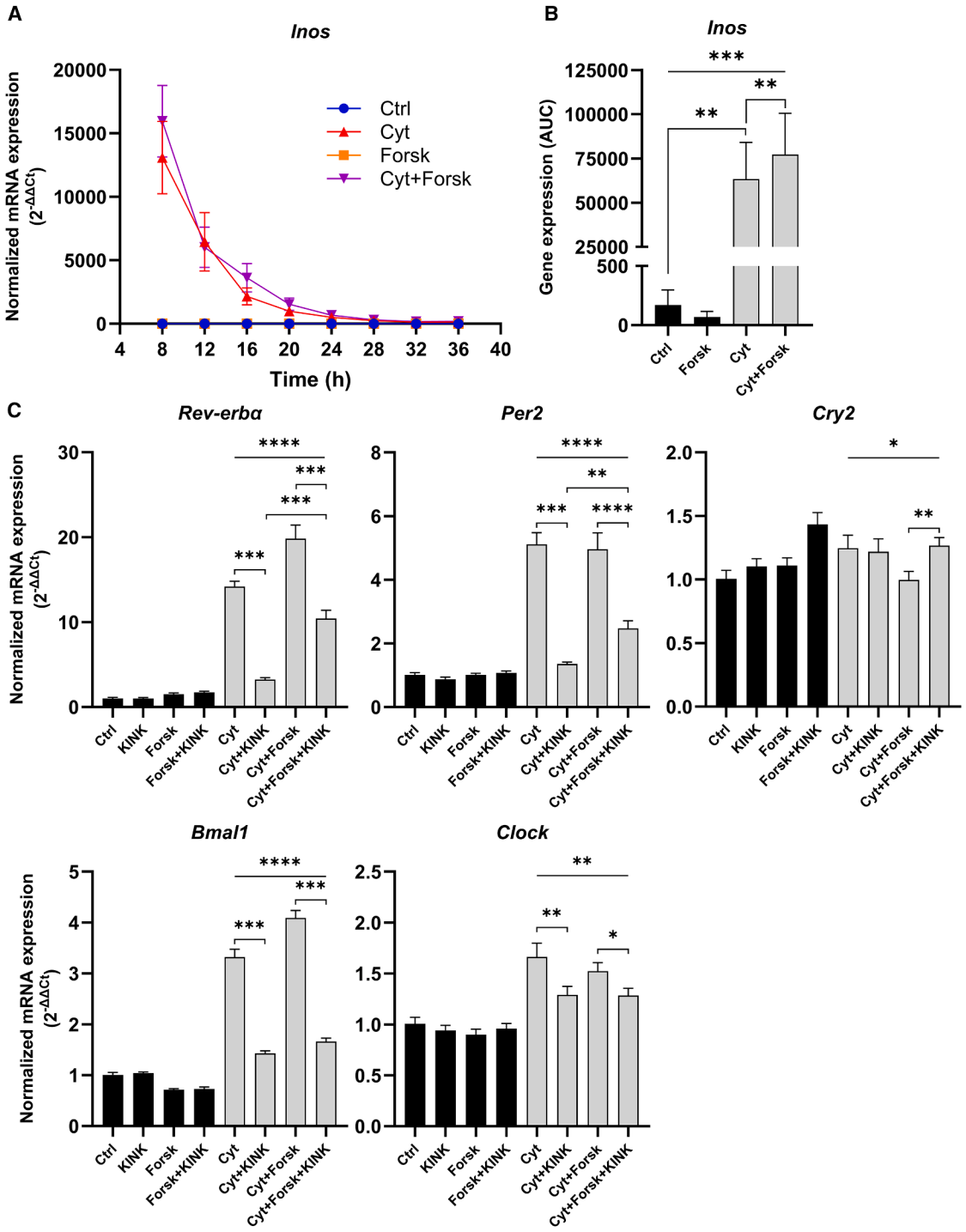

Figure 4. Synchronization potentiates proinflammatory cytokine-induced *Inos* expression, and NF-κB inhibition differentially reverses proinflammatory cytokine modulation of core clock gene expression

INS-1 cells were handled as described in Figure 1. Normalized mRNA expression was calculated using *Hprt1* and 5s rRNA as reference genes.

(A) Time-dependent normalized mRNA expression.

(B) AUC of the curves in (A).

(legend continued on next page)

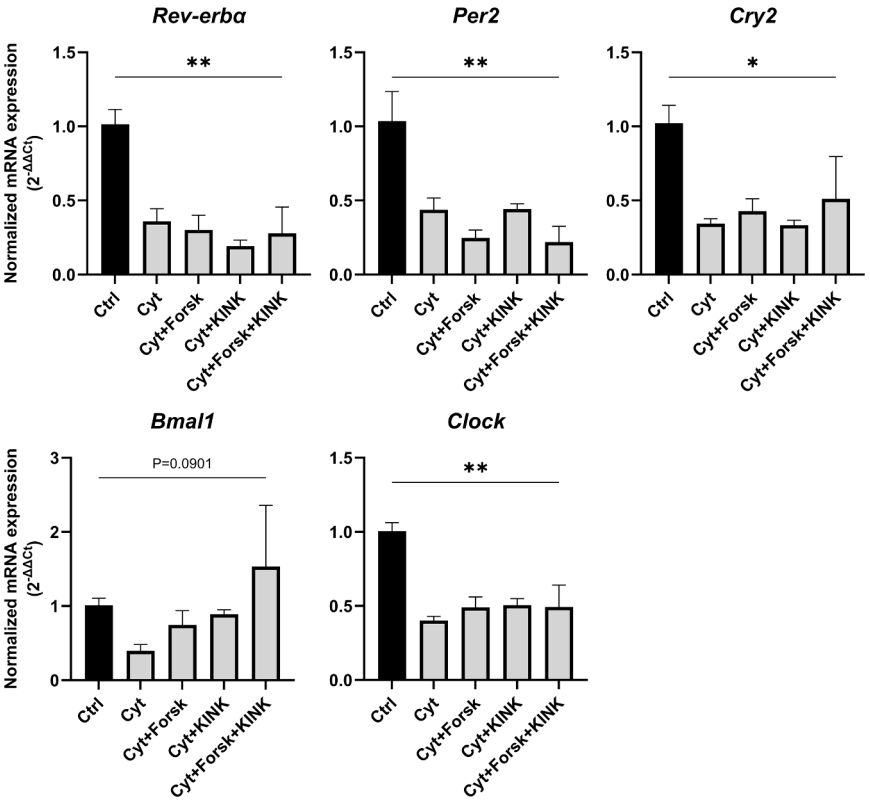

Figure 5. Cytokines reduce core clock mRNA expression in intact murine islets independently of synchronization status and NF-κB activity

Intact murine islets, non-synchronized or synchronized with a 1-h forskolin pulse, were cultured for 12 h in the presence (Cyt) or absence (Ctrl) of 300 pg/mL of mIL-1β and 0.2 ng/mL rIFN-γ. Islets were either pre-incubated with 1 μM KINK-1 (KINK) or vehicle for 1 h, and exposed to KINK-1, together with the aforementioned conditions, as described in the STAR Methods. Normalized mRNA expression was calculated using *Hprt1*, *Ppia,* and *Rplo* as reference genes. Data are presented as means ± SEM (N = 3–4, except for *Per2* Cyt and Cyt+Forsk+KINK where *N* = 2 due to missing values). Statistics are one-way ANOVA, with significance levels annotated as follows: * = *p*-value <0.05 and ** = *p*-value <0.01.

to the extrinsic (death domain) apoptotic pathway.[18] Cytokine exposure of synchronized cells was associated with increased activity of intrinsically activated Caspase 9 but not extrinsically activated Caspase 8 activity (Figure S8A), resulting in a small but significant increase in cytotoxicity (apoptosis and late apoptotic necrosis) (Figures S8B and S8C).

In summary, synchronization modestly potentiates the cytokine-mediated activation of ER stress and the intrinsic apoptotic pathway in INS-1 cells. Although changes were statistically significant, these modest differences are not likely of biological importance.

NF-κB inhibition differentially affects cytokine toxicity in a cytokine concentration-dependent manner in INS-1 cells

Having demonstrated the importance of NF-κB signaling in cytokine-mediated clock gene transcript and ind-proteasomal subunit expressions as well as in the effects of synchronization on β-cell viability, we next tested the role of NF-κB in cytokine-mediated cytotoxicity in insulin-producing cells.

In the absence of cytokines, synchronized cells were more viable than their non-synchronized counterpart, and KINK-1 attenuated this advantage, albeit not completely (Figure S9). We next verified that NF-κB inhibition reduced cytokine-mediated cytotoxicity in the INS-1 *Per2:Luc* reporter cells exposed to varying IL-1β concentrations with a fixed IFN-γ concentration. Indeed, KINK-1 reduced the IL-1β dose- and time-dependent increase in apoptosis and post-apoptotic necrosis in both non-synchronized and synchronized cells (Figures 7A, 7B, and S9). At 10 pg/mL IL-1β KINK-1 increased cytotoxicity in non-synchronized cells, suggesting a protective role of NF-κB at low IL-1β concentrations in these cells, while KINK-1 reduced cytotoxicity in synchronized cells (Figure S9). While the effects of synchronization and NF-κB inhibition were neutral at 15 pg/mL of IL-1β, synchronization potentiated cytokine-induced apoptosis and late apoptotic necrosis at 30 pg/mL (Figures 7 and S9).

We intended to verify key findings from the above experiments in the human EndoC-βH3 cell line.[35] However, even at much higher cytokine concentrations, these cells were not cytokine-sensitive (data not shown).

Synchronization prevents cytokine-induced cytotoxicity, but not Inos mRNA expression, whereas NF-κB inhibition prevents both cytotoxicity and Inos mRNA expression in murine islets

Since the clock gene transcriptional responses to cytokines differed between β-cells and intact islets, we reasoned that the action of cytokines on intact murine islet viability might also differ. As expected, IL-1β and IFN-γ induced cytotoxicity in a time-dependent manner in non-synchronized islets, associated

(C) Cells were additionally pre-incubated with 1 μM KINK-1 (KINK) for 1 h, and exposed to the inhibitor, together with the aforementioned conditions for the 16-h duration of the experiment. Normalized mRNA expression was calculated using *Hprt1* and 5s rRNA as reference genes. Data are presented as means ± SEM (*N* = 4). Statistics are repeated measurements ANOVA with Holm-Sidak's multiple comparisons test. Overall ANOVA *p*-value represented by symbols above the top line, while the brackets annotate comparisons. Significance levels are annotated as follows: * = *p*-value <0.05, ** = *p*-value <0.01, *** = *p*-value <0.001, and **** = *p*-value <0.0001. See also Figures S5 and S6.

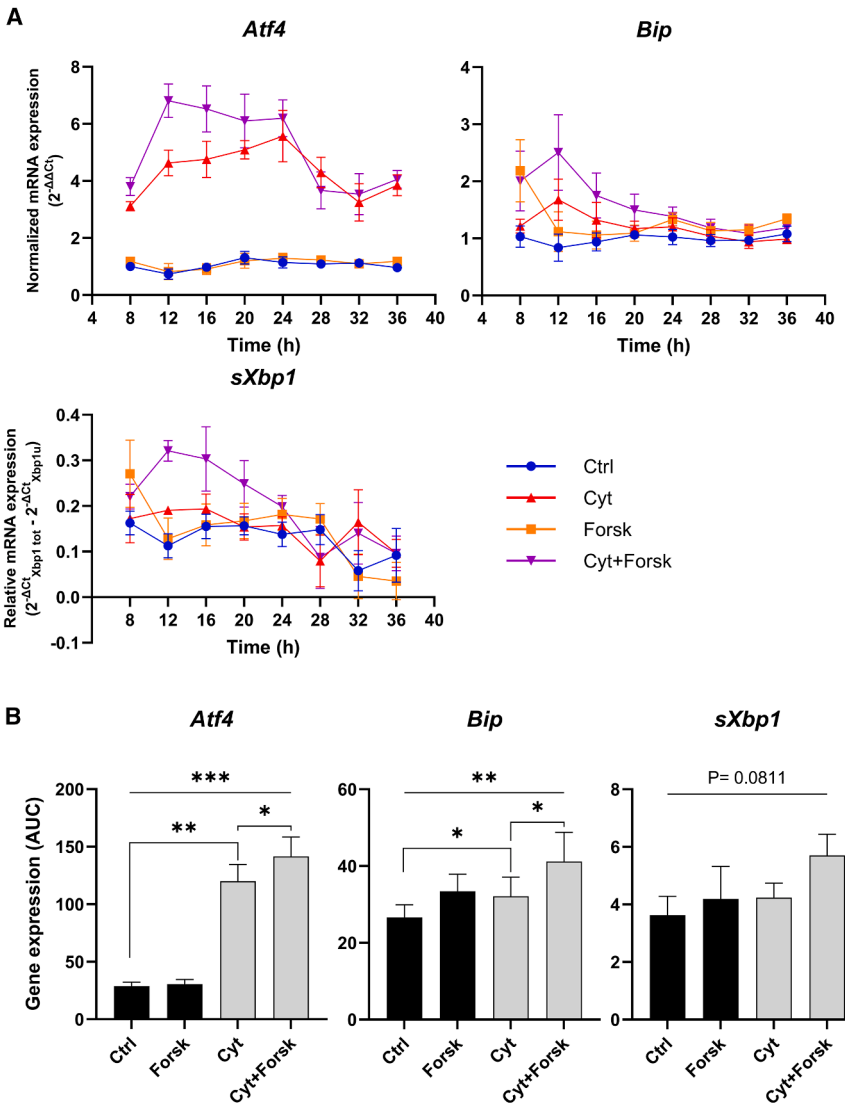

Figure 6. Synchronization potentiates the proinflammatory cytokine-mediated increases in ER stress-associated genes

INS-1 cells were handled as described in Figure 1. Normalized mRNA expression was calculated using *Hprt1* and 5s rRNA as reference genes.

(A) Time-dependent normalized mRNA expression.

(B) AUC of the curves in (A). Data are presented as means ± SEM (N = 4). Statistics are repeated measurements ANOVA with Holm-Sidak's multiple comparisons test. Overall ANOVA p-value represented by symbols above the top line, while the brackets annotate comparisons. Significance levels are annotated as follows: * = p-value <0.05, ** = p-value <0.01, and *** = p-value <0.001. See also Figure S7.

with increased *Inos* expression after 12 h of cytokine exposure (Figure 8), both of which were prevented by NF-κB inhibition, as reported earlier. Interestingly, in murine islets, synchronization prevented cytokine-mediated cytotoxicity to a degree equaling that of KINK-1 (Figures 8A and 8B), but not *Inos* expression (Figure 8C). Accordingly, NF-κB inhibition did not further reduce cytokine-induced toxicity, but did completely block *Inos* expression similarly in synchronized and non-synchronized islets. Taken together, these observations suggest that synchronization protects against toxicity in murine islets by an NF-κB independent mechanism.

NF-κB inhibition differentially affects cytokine-mediated changes in period and acrophase in a cytokine concentration-dependent manner in INS-1 cells

We next wished to investigate the dose-dependent effect of cytokines and NF-κB inhibition on circadian parameters using the INS-1 *Per2:Luc* reporter cells (Figures 9, S10, and S11). Non-detrended traces demonstrated that high concentrations of IL-1β (30 and 60 pg/mL) reduced *Per2:Luc* bioluminescence at 96 h, with the decrease starting after approx. 10 h, which was reversed by KINK-1 (Figure S10). This reduction was associated with a decrease in *Per2* promotor-driven *Luc* mRNA at 20 h, but not in *Per2* mRNA (Figure S12), suggesting that the decreased bioluminescence signal is indeed due to reduced expression of luciferase as an expression of general effects on circadian rhythmicity, concurrent with the increased *Per2* expression which would provide a repressive function on the core clock. Hence, the reduced bioluminescence signal is not an artifact caused by a global effect of cytokine toxicity, but an expression of circadian amplitude. This notion was supported by the intact oscillations (Figures 9 and S10) and the toxicity data (Figure 7).

Non-synchronized cells displayed inherent rhythmicity (Figure 9A) from which acrophase (∼20 h) (Figure 9B) and period (∼27 h) (Figure 9D) could be determined after detrending. Indeed, entrainment by forskolin markedly altered the rhythmicity of INS-1 cells closer to an expected circadian period (Figures 9B and 9D) (acrophase and period both ∼25 h). Interestingly, cytokines dose-dependently advanced the acrophase to ∼20 h and prolonged the period to ∼30 h in synchronized but not in non-synchronized cells (Figures 9C and 9E). Notably, NF-κB inhibition normalized the cytokine-modulation of acrophase and period in synchronized INS-1 *Per2:Luc* cells at low (≤15 pg/mL) IL-1β concentrations.

At 30 pg/mL of IL-1β, KINK-1 failed to reverse the cytokine-mediated period lengthening, yet synchronized cells maintained a rhythmic profile of the detrended traces (Figure 10). At 60 pg/mL, no further period lengthening was observed, coinciding with plateauing of the maximal cytotoxic response (Figure 7A). For synchronized cells exposed to 60 pg/mL IL-1β and KINK-1,

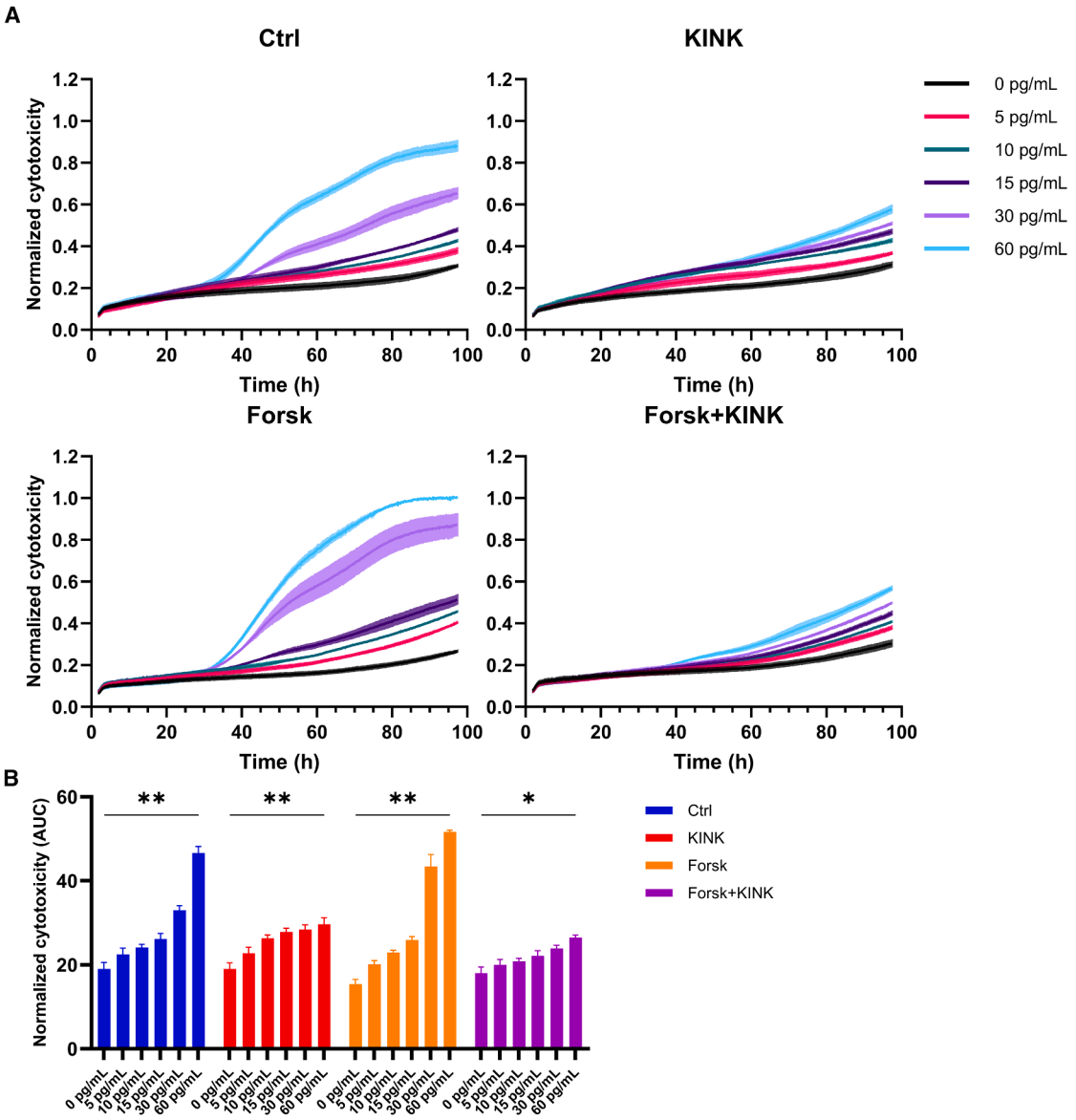

Figure 7. NF-κB inhibition reduces the dose-dependent proinflammatory cytokine-mediated cytotoxicity in both synchronized and non-synchronized cells, while synchronization modifies cytokine-mediated cytotoxicity dependent on cytokine concentration

INS-1 *Per2:Luc* cells were cultured in the presence of varying concentrations of mIL-1β (legend) and 0.1 ng/mL rIFN-γ. Cells were synchronized with a 1-h 10 μM forskolin pulse (Forsk), as well as 1 μM KINK-1 (KINK) in a 1-h preincubation and for the duration of the experiment. Cells not exposed to forskolin or KINK-1 have been annotated as control (Ctrl).

(A) Cytotoxic response normalized to the overall maximum signal obtained. Cytotoxicity was monitored in real-time at 10-min intervals for 96 h. Significant difference between Ctrl 30 pg/mL and Forsk 30 pg/mL (two-tailed paired Student's *t* test $p = 0.0327$).

(B) AUC of the normalized cytotoxicity response. Data are presented as means ± SEM ($N = 3$). Statistics are repeated measurements one-way ANOVA with *p*-values represented by symbols above the line (B). Significance levels are annotated as follows: * = *p*-value <0.05 and ** = *p*-value <0.01. See also Figure S9.

the period length reached the upper limit (34 h) of the period length window used in the analysis (18–34 h) (Figure 10D, dotted line), with a flat profile of the detrended trace (Figure 10C), indicating that rhythmicity in synchronized cells treated with KINK-1 in the presence of 60 pg/mL of IL-1β was lost or had become infradian. Interestingly, these cells still suffered less apoptosis and post-apoptotic necrosis than cells not treated with the NF-κB inhibitor (Figures 7A and 7B), suggesting a protective effect of NF-κB inhibition against cytokine toxicity uncoupled from clock rescue.

In summary, IL-1β and IFN-γ dose-dependently advance acrophase and lengthen the period in the non-cytotoxic cytokine concentration range in an NF-κB dependent manner. In contrast, at cytotoxic cytokine concentrations, the increased period

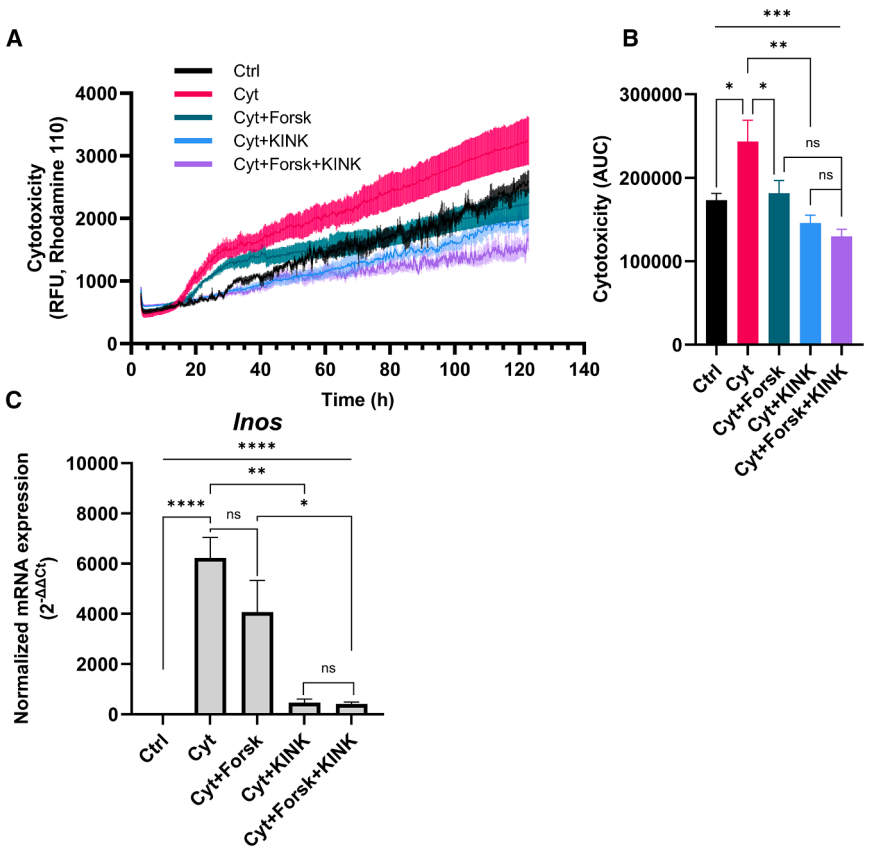

Figure 8. Synchronization prevents cytokine-induced cytotoxicity, but not Inos mRNA expression, whereas NF-κB inhibition prevents both cytotoxicity and Inos mRNA expression in murine islets

(A) Murine islets were cultured as described in Figure 5 and the cytotoxicity response was monitored as apoptosis and late apoptotic necrosis.

(B) AUC of the cytotoxicity response.

(C) Islets were exposed for 12 h before harvest, as described in Figure 5. Normalized *Inos* mRNA expression was calculated using *Hprt1*, *Ppia,* and *Rplo* as reference genes. Data are presented as means ± SEM (*N* = 4 for A and B, N = 3–4 for C). Statistics is one-way ANOVA with Holm-Sidak's multiple comparisons test. Overall ANOVA *p*-values are represented by symbols above the top line, while the brackets annotate comparisons. Significance levels are annotated as follows: ns = not significant, * = *p*-value <0.05, ** = *p*-value <0.01, *** = *p*-value <0.001, and **** = *p*-value <0.0001.

length plateaus, with NF-κB inhibition being unable to reverse this effect and causing loss of circadian rhythmicity.

NF-κB inhibition does not prevent cytokine-induced period lengthening and acrophase delay in synchronized murine islets

We observed that synchronization differentially affected cytokine-induced changes in clock gene transcription and viability in insulin-secreting INS-1 cells compared to intact mouse islets. Since these differences depended on NF-κB involvement, we next interrogated if NF-κB regulates cytokine-mediated circadian rhythmicity monitored by continuous bioluminescence recording in synchronized islets isolated from *mPer2:Luc* reporter mice (Figure 11). Exposure to cytokines led to increased circadian period length and delayed acrophase in synchronized islets, in concordance with our previous report.[24] Of note, these changes were unaffected by NF-κB inhibition, underpinning the notion that cytokine-induced toxicity and clock perturbation depend on different mechanisms in a β-cell line and intact murine islets.

DISCUSSION

Our finding that a combination of proinflammatory cytokines, IL-1β and IFN-γ, alters the expression level of several core clock components at the protein level expands our earlier reporting of cytokine-induced changes in the transcription of these components in INS-1 cells.[24] This observation is important for a comprehensive interpretation of how cytokines regulate the transcriptional-translational feedback loop in the clock machinery, as clock proteins are the transcriptional repressors and activators. Since the previous intriguing observations were obtained in a non-synchronized cell system, we here investigated cytokine regulation of clock components at both the transcriptional and translational level in a forskolin-synchronized cell model.

We demonstrate that circadian synchronization of INS-1 cells significantly potentiated cytokine-mediated alterations of the transcription of several core clock genes and, interestingly, the level of a more restricted repertoire of clock proteins (the activator CLOCK and the repressor REV-ERBα). Since circadian dynamics depend on proteasomal degradation of clock proteins, we anticipated parallel regulation of proteasomal components. Synchronization did indeed potentiate the cytokine-induced transcription of the ind-proteasomal subunits *Psmb8* and *Psmb9* in INS-1 cells.

Further mechanistic studies revealed that synchronization of INS-1 cells potentiated the cytotoxic effect of proinflammatory cytokines in a cytokine dose-dependent manner, associated with potentiation of ER stress markers, *Inos* mRNA expression, and increased Caspase 9 activity. We reasoned that cytokine-triggered NF-κB signaling might be a unifying signaling pathway conveying synchronization-dependent potentiation of cytokine-regulation of clock and ind-proteasomal component expression, as well as the summarized mechanistic pathways in INS-1 cells. Indeed, pharmacological inhibition of NF-κB activity reverted the cytokine-mediated alterations in clock gene expression in both non-synchronized and, to a lesser extent, synchronized INS-1 cells, associated with reduced cytotoxicity. In accordance with the known bimodal effect of proinflammatory cytokines on

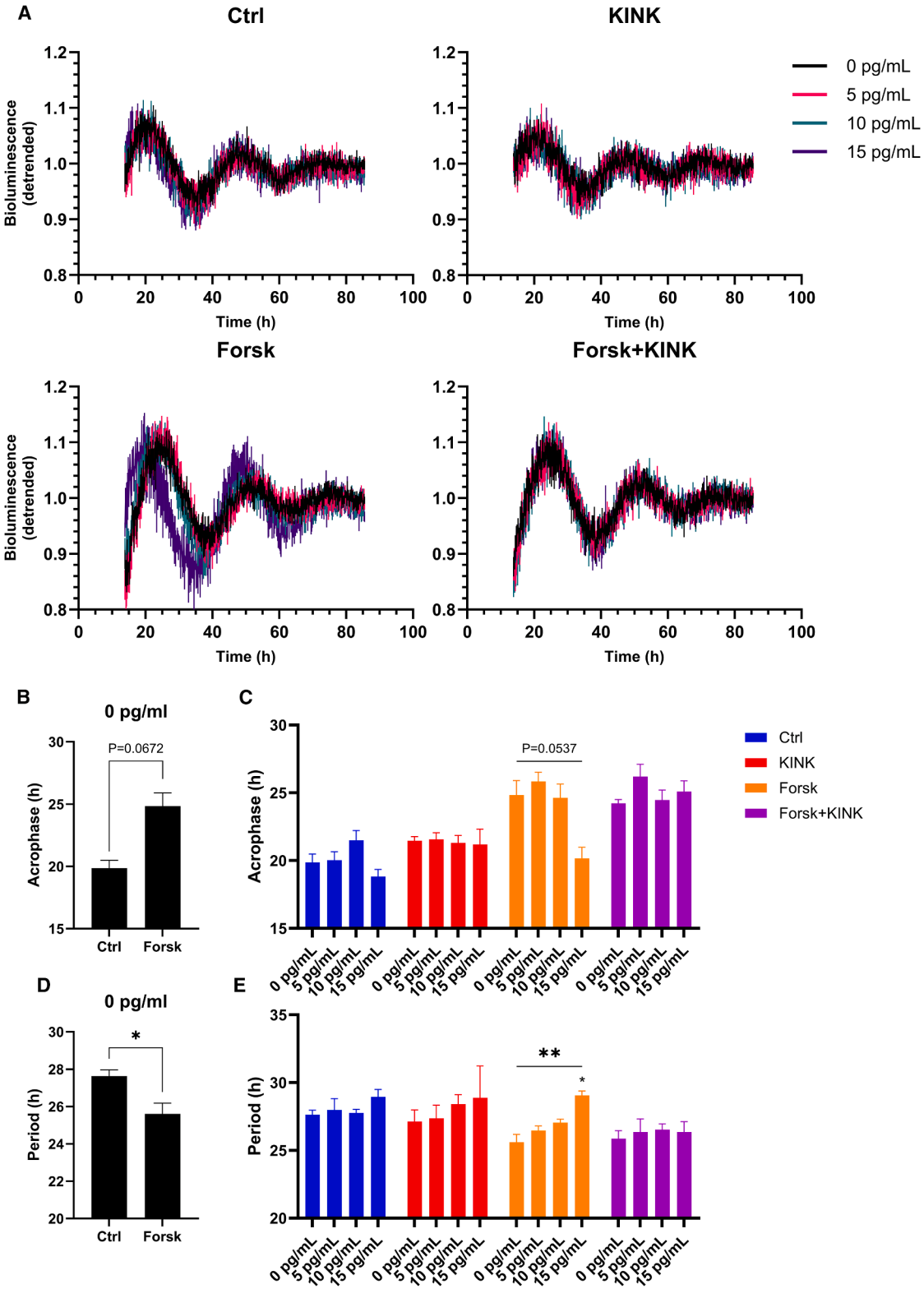

(legend on next page)

β-cell function and viability,[36,37] NF-κB inhibition normalized acrophase advancement and period lengthening caused by low (≤15 pg/mL) IL-1β in INS-1 cells. At high (≥30 pg/mL) IL-1β, NF-κB inhibition failed to revert period lengthening and resulted in loss of circadian rhythmicity in these cells.

Taken together, our data suggest that proinflammatory cytokines perturb the circadian clock in an NF-κB dependent manner in INS-1 cells and that clock perturbation desensitizes these insulin-producing cells to cytokine-mediated assault.

The observation that NF-κB is crucial for both the cytokine-mediated uncoordinated change in clock gene expression and in perturbing circadian rhythmicity in INS-1 cells supports our earlier findings that cytokine-activation of multiple pathways downstream of NF-κB in these cells is associated with the cytokine-mediated change in core clock gene expression profile.[24] The involvement of NF-κB signaling in core clock gene expression is supported by the observation that multiple clock genes have NF-κB binding sites. Importantly, p65 displays an oscillatory protein expression and activity profile, required for circadian oscillations of core clock genes and proteins in non-cytokine exposed mouse embryonic fibroblasts (MEFs), and a functional IKK complex is required for mouse locomotor rhythms.[22,23,38] In synchronized human U2OS cells, upregulation of p65 shortened period length, while inhibition increased period length, indicative of an inhibitory function by p65 on BMAL1-CLOCK transcriptional activity, similar to the repressor function of CRY1.[23] This contrasts with our findings that NF-κB inhibition in non-cytokine-exposed synchronized INS-1 cells did not change rhythmic parameters, and inhibition of NF-κB in cytokine-exposed synchronized cells shortened the period. The discrepancy could indicate cell-specific differences in NF-κB action as reflected, for example, by the anti-apoptotic action of NF-κB in the liver vs. the pro-apoptotic effects in the β-cell.[39,40] A cell-specific NF-κB action is further illustrated in murine liver, where lipopolysaccharide (LPS) exposure increases p65 binding and activity, resulting in inhibition of clock repressors, but not activators,[22] in contrast to the general NF-κB dependent upregulation observed in our study. Additionally, LPS exposure results in genome-wide relocalization of BMAL1-CLOCK to sites in proximity to genes involved in inflammatory and metabolic signaling and apoptosis and is dependent on functional p65.[22] This concept may explain the NF-κB-dependent cytokine-mediated effects on BMAL1-CLOCK-controlled genes shown here in INS-1 cells.

Interestingly, the rescue potential of NF-κB inhibition on rhythmic parameters in INS-1 cells depended on the IL-1β concentration. At non-toxic cytokine concentrations, incapable of altering clock gene expression in non-synchronized cells (≤15 pg/mL IL-1β),[24] NF-κB inhibition reversed cytokine-mediated alterations in rhythmicity (Figures 7 and 9). In contrast, at higher cytotoxic levels of IL-1β (≥30 pg/mL), NF-κB inhibition restrained the reintroduction of a rhythmic behavior, while still reducing cytokine-mediated cytotoxicity (Figures 7 and 10). The uncoupling of the effects of the KINK-1 inhibitor on clock perturbation and toxicity may be caused by the global NF-κB inhibiting activity of KINK-1, unselective for NK-κB homo- or heterodimers, the balance of which may fine-tune the cellular responses to inflammatory stimuli.

Synchronized INS-1 cells exposed to high cytokine concentrations in the absence of the NF-κB inhibitor were capable of reintroducing rhythmicity after the first ∼30 h of non-rhythmic behavior, coinciding with the uncoordinated clock transcriptional changes (Figure 1) reversible by NF-κB inhibition (Figures 4 and S5), possibly as a defensive response.

The toxic effects of the cytokine concentrations and exposure durations raise the question of whether these effects relate to physiological situations or are an artifact of the cell culture. The determination in bodily fluids of low concentration cytokines, such as IL-1β, the driving cytokine here, is technically challenging due to an abundance of IL-1 binding proteins in these fluids. However, studies that have reproducibly measured IL-1 in plasma report levels of 120 pg/mL in septic patients,[41] thus very similar to the 150 pg/mL used here. Similar concentrations were reported in synovial fluid of osteoarthritis patients[42] but 100 times higher (17 ng/mL) in fluid from rheumatoid arthritis patients.[43] Considering the dilution factor and interfering binding proteins in the above studies, it is likely that IL-1 concentrations in the "immunological synapse" between IL-1-producing cell and target β-cell will attain even higher concentrations. Thus, the concentrations used here are in the low range in the pathophysiological spectrum.

The potential involvement of the ind-proteasome in regulation of the circadian transcriptional-translational feedback loop is supported by our earlier observation that inhibiting the ind-proteasome reverses the cytokine-mediated effects on INS-1 cell clock gene expression.[24] Taken together with the observation that the ind-proteasome is constitutively expressed and active in β-cells and that the activity of the ind-proteasome is induced by IFN-γ or low concentrations of IL-1β,[44,45] our data suggests that the ind-proteasome regulates the dynamics of the molecular β-cell clock, an action potentiated by synchronization. This notion is exemplified by the discrepancy between *Bmal1* mRNA and protein (Figures 1 and 2).

REV-ERBα mRNA and protein expressions were cytokine-coregulated and potentiated by synchronization in INS-1 cells. Pharmacological activation of REV-ERBα impairs autophagy and insulin expression and secretion while promoting apoptosis in β-cells, likely through clock-independent transcriptional effects.[24,46] The loss of β-cell function and increased apoptosis might be an effect of impaired autophagy, as loss of autophagy

Figure 9. NF-κB inhibition normalizes the dose-dependent proinflammatory cytokine-mediated changes in acrophase and period

INS-1 *Per2:Luc* cells were handled as described in Figure 7.

(A) Detrended *Per2:Luc* bioluminescence signal, recorded at 10-min intervals presented in the functional window (13.5–85.5 h) of the analysis, from which acrophase in the absence (B) and presence (C) of cytokines, in addition to period in the absence (D) and presence (E) of cytokines, have been determined. Data are presented as means ± SEM ($N = 3$). Statistics are two-tailed paired Student's t test for (B) and (D), and repeated measurements one-way ANOVA with p-values represented by symbols above the line and with Dunnett's multiple comparisons test to 0 pg/mL for (C) and (E). Significance levels are annotated as follows: * = p-value <0.05 and ** = p-value <0.01. See also Figures S10–S12.

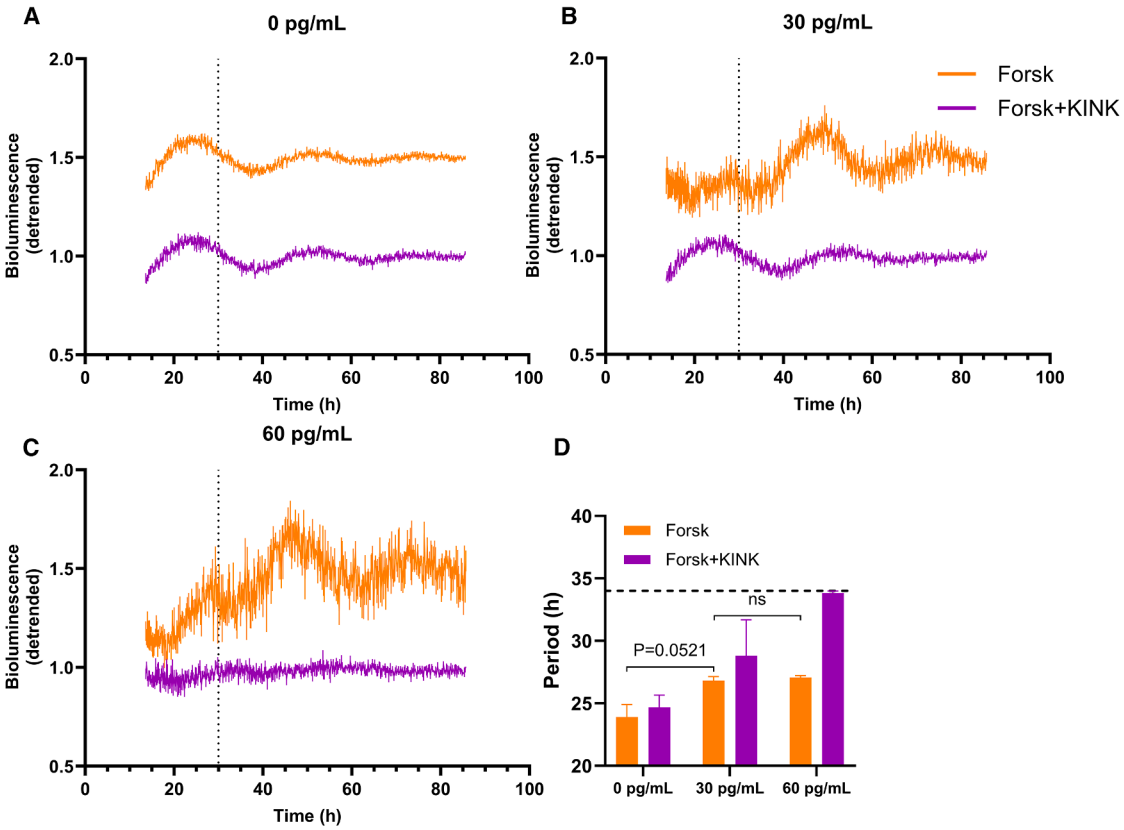

Figure 10. NF-κB inhibition fails to normalize period length at cytotoxic IL-1β concentrations

(A–C) INS-1 *Per2:Luc* cells were synchronized with a 1-h 10 μM forskolin pulse (Forsk) and 1 μM KINK-1 (KINK) in a 1-h preincubation and for the duration of the experiment. Cells were cultured in the absence (A) presence of 30 (B) or 60 (C) pg/mL mIL-1β with 0.1 ng/mL rIFN-γ, with bioluminescence recorded at 10-min intervals and data detrended.

(D) Period length of (A–C). Period length was determined using detrended data in an analysis window between 30 and 85 h (vertical dotted line, A–C), with an estimated period length between 18 and 34 h (horizontal dotted line, D). Data are presented as means ± SEM ($N = 3$). Statistics are repeated measures one-way ANOVA. Significance levels are annotated as follows: ns = not significant.

results in loss of β-cell mass in mice.[47] Accordingly, REV-ERBα/β agonists impair autophagy and induce apoptosis in a range of cancer cells,[48] supporting REV-ERBα/β′s role in apoptosis. Thus, the potentiated cytokine-mediated cytotoxicity during synchronization could in part be explained by the potentiated expression levels of REV-ERBα in synchronized INS-1 cells. However, it cannot be rejected that these REV-ERBα mediated effects are clock-independent.

The widely used 1-h forskolin-pulse was used here as a synchronization stimulus, shown to upregulate *Per1/2* in INS-1 cells[24] which is known to result in entrainment of the molecular clock.[28] Forskolin elevates cAMP, which increases Protein kinase A (PKA) activity, resulting in Ca^{2+}/cAMP responsive element binding protein (CREB) activity, and thereby *Per1/2* expression,[28] but also of numerous other genes. We do not believe that our observations are confounded by off-clock target effects, for the following reasons. First, cAMP has a half-life of <1 ½ minutes,[49] resulting in a very transient increase in cAMP after a 1-h forskolin pulse. This is supported by the observation that insulin secretion from murine islets exposed to 10 μM IBMX and 1 μM forskolin increased ∼350% during a 40-min exposure, but normalized 30 min after the cessation of IBMX and forskolin exposure,[50] indicating that cAMP turnover in β-cells is very fast to enable minute-by-minute adjustments in insulin secretion. As cytokine-mediated β-cytotoxicity is observed after 24–96 h, it is unlikely that these effects are due to constant high cAMP levels. In fact, cAMP protects β-cells against apoptosis,[51] similar to what is seen in the current study in the absence of proinflammatory stress. Second, cAMP can inhibit and promote NF-κB signaling, depending on stimulus and cell type.[52] However, in non-cytokine exposed cells, NF-κB signaling in INS-1 cells was unchanged at 1 h[24] and 3 h (data not shown) post-forskolin pulsing, supporting that the potentiating effects of synchronization on cytokine-action are not due to off-target effects secondary to transiently increased cAMP.

In murine islets, cytokines generally inhibited levels of circadian activator and repressor mRNAs independently of synchronization status or NF-κB activity, in contrast to the observations in INS-1 cells, but in a non-antiphasic pattern analogous to the findings in INS-1 cells. At this transcriptional "setting" of the clock, synchronization prevented cytokine-mediated cytotoxicity, but not *Inos* expression, in islets. Remarkably, the

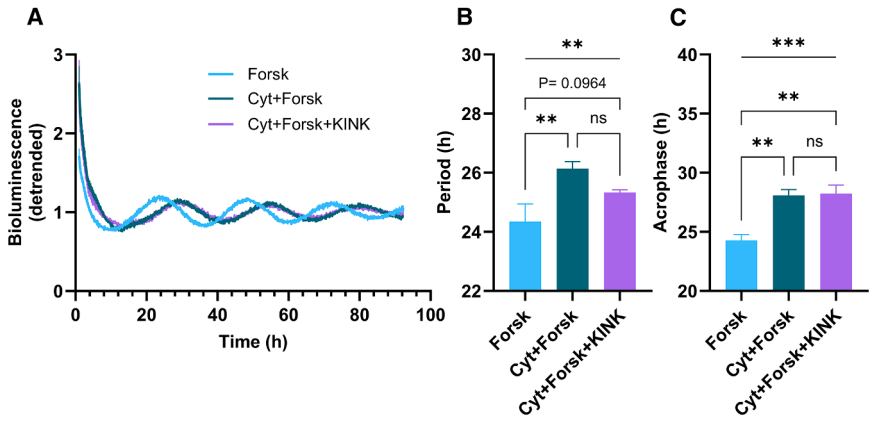

Figure 11. Cytokines alter rhythmic parameters in reporter islets independent of NF-κB activity

mPer2:Luc reporter islets were synchronized with a 1-h forskolin pulse (Forsk), and exposed to either 300 pg/mL of mIL-1β and 0.2 ng/mL rIFN-γ alone (Cyt) or in combination with 1 μM KINK-1 (KINK). (A) Detrended *Per2:Luc* bioluminescence signal, recorded at 10-min intervals, with calculated period (B) and acrophase (C). Data are presented as means ± SEM (N = 5–8). Statistics are ordinary one-way ANOVA with Tukey's multiple comparisons test. Overall ANOVA *p*-value is represented by symbols above the top line, while the brackets annotate comparisons. Significance levels are annotated as follows: ns = not significant, ** = *p*-value <0.01, and *** = *p*-value <0.001.

anti-apoptotic action of synchronization equaled that of NF-κB inhibition. Accordingly, the KINK-1 inhibitor did not further reduce cytokine-induced toxicity but completely blocked *Inos* expression as in non-synchronized islets. Cytokines increased period length and delayed acrophase in synchronized islets, and these changes were unaffected by NF-κB inhibition.

The data obtained with INS-1 cells and murine islets thus differ in three regards: (1) The opposite cytokine effect on core clock component mRNA transcription, (2) the different effects of synchronization on clock mRNA expression and apoptosis, and (3) the differential role of NF-κB in these outcomes. There are several hypothetical explanations for these divergent observations: (1) The biosociology of the model system. The paracrine and adhesion-molecule dependent cell-to-cell interaction and 3D-architecture of the intact islet ensure optimal physiological function of the endocrine pancreas, witnessed by the impaired insulin-secretion from dissociated and sorted β-cells that are rescued by glucagon supplementation.[53] In addition, circadian regulation and rhythmicity of gene expression, including that of inflammatory agonists and antagonists, differ remarkably between islet cell subpopulations.[30] Taken together, the resultants of cytokine-mediated clock perturbation on pancreatic endocrine cell fate may be modified by the integrated interaction of β-cells and non-β-cells in the intact islets, lacking in insulin-producing cell lines. (2) Species-dependent cytokine sensitivity. A cytokine sensitivity hierarchy exists between the most widely used *in vitro* models of endocrine pancreatic cells, with rat being more sensitive than mouse being more sensitive than human cells. Accordingly, cytokine-induced cytotoxicity and gene transcription are to a large extent NO-dependent in rat, but less so in murine and human models, despite similar inducibility of *Inos*[54–56]. (3) Differentiation level of the *in vitro* model. De-differentiation, e.g., by nuclear exclusion of β-cell specific transcription factors such as *Pdx-1,* is a general defense mechanism in stressed β-cells, and protects against cytokine assault.[57,58] Since the INS-1 cell line is by nature de-differentiated, the responses to synchronization would be expected to differ from fully differentiated intact islet cells. (4) Differences in culture conditions. Although we aimed at comparable exposures and culture conditions by pilot experiments, it is possible that the higher concentrations of cytokines chosen to yield comparable outcomes to those seen in INS-1 cells may not have hit the same point on the steep dose-response relationship characteristic of β-cell cytokine responses. Irrespective of the causes of the different results observed between models, the observation that the direction of change of clock-gene transcriptome is associated with different but consistent cell outcomes yields novel insight into the complex interplay between cell stress, clock setting, and cell fate that warrants further investigation, and not only in pancreatic islets.

Finally, with regard to the differential role of NF-κB in the two *in vitro* models, we speculate that the proinflammatory transcriptional activity of NF-κB in synchronized INS-1 cells is enhanced by interaction with clock transcription factors, as it has been suggested for the clock activator *BMAL1*.[22] In murine islets, although we confirmed the critical role of NF-κB in cytokine-mediated apoptosis, NF-κB independent pathways must be engaged in mediating cytokine effects on clock gene transcription and circadian rhythmicity in murine islets. These pathways should be explored since the rescue potential of clock synchrony equaled that of NF-κB in magnitude.

In conclusion, circadian synchronization differentially modifies cytokine-mediated transcriptomic remodeling and cell death in insulin-producing cells and intact mouse islets, depending on the involvement of NF-κB signaling.

Limitations of the study

A major strength of the methodological approach in this study was the use of extended real-time assay to monitor both circadian rhythmicity, employing reporter INS-1 cells and murine islets, and cytotoxicity. In INS-1 cells this was even multiplexed for the same cultures, giving insight into the association between rhythmicity and cytotoxicity. In combination with extensive qPCR and western blotting verification of fluctuations in core clock components, these assays enabled interpretation of descriptive and mechanistic data. A weakness is the lack of data from human islet cells. The potential use of the human β-cell line EndoC-βH3 was explored in this study but had to be abandoned since these cells were found to be unresponsive to proinflammatory cytokines, a problem also encountered by other laboratories (Soleimanpour S, personal communication). Thus, our observations should be repeated in human islets.

RESOURCE AVAILABILITY

Lead contact

Further information and requests for resources and reagents should be directed to and will be fulfilled by the lead contact, Phillip Alexander Keller Andersen (phillip.andersen@sund.ku.dk).

Materials availability

This study did not generate new unique reagents or material.

Data and code availability

- This paper does not report original code.
- Data and any additional information required to reanalyze the data reported in this paper is available from the lead contact upon request.

ACKNOWLEDGMENTS

We thank Frederik Vilhardt and Jonas Hyld Steffen (University of Copenhagen, Copenhagen, Denmark) for their invaluable help in establishing the INS-1 *Per2:Luc* cell line. We further thank Loïc Metz (Dept. of Biomedical Sciences, University of Copenhagen) and Volodymyr Petrenko (University of Geneva, Geneva, Switzerland) for technical assistance and helpful discussions. This study was funded by the Independent Research Fund Denmark (grant nos. 8020-00359B and 1030-00076B), the Danish Cardiovascular Academy (funded by the Novo Nordisk Foundation (grant no. NNF20SA0067242) and the Danish Heart Foundation)), the Novo Nordisk Foundation (grant no. NNF21OC0070345), and Prins Bernhard Cultuurfonds (grant no. 40042732). C.D. was funded by SNSF grant no. 310030-219187, the Vontobel Foundation, the Olga Mayenfisch Foundation, the Novartis Consumer Health Foundation, Ligue Pulmonaire Genevoise, Swiss Cancer League (KFS-5266-02-2021-R), the Velux Foundation, the ISREC Foundation, SACAD, and the Gertrude von Meissner Foundation. G.K. was funded by the Nova Foundation (Fondation pour l'innovation sur le cancer et la biologie) and Swiss Life Foundation. Graphical abstract was created in BioRender, https://BioRender.com/ki75g2n.

AUTHOR CONTRIBUTIONS

Conceptualization, P.A.K.A. and T.M.P.; methodology, P.A.K.A., R.H.R., A.F.L., C.J.S., C.D., and G.K.; formal analysis, P.A.K.A., R.H.R., I.S., E.B.O., G.K., and C.J.S.; investigation, P.A.K.A., R.H.R., I.S., E.B.O., G.K., C.J.S., E.Z.S., and A.F.L.; writing – original draft, P.A.K.A. and T.M.P.; writing – review and editing, P.A.K.A., R.H.R., I.S., E.B.O., G.K., C.J.S., E.Z.S., A.F.L., C.D., and T.M.P.; visualization preparation, P.A.K.A., R.H.R., I.S., E.B.O., and G.K.; Supervision, P.A.K.A., G.K., A.F.L., C.D., and T.M.P; project administration, P.A.K.A., A.F.L., C.D., and T.M.P.; funding acquisition, R.H.R., I.S., G.K., E.Z.S., A.F.L., C.D., and T.M.P..

DECLARATION OF INTERESTS

The authors declare no competing interests.

STAR★METHODS

Detailed methods are provided in the online version of this paper and include the following:

SUPPLEMENTAL INFORMATION

Supplemental information can be found online at https://doi.org/10.1016/j.isci.2025.112431.

Received: April 17, 2024
Revised: January 30, 2025
Accepted: April 10, 2025
Published: April 15, 2025

REFERENCES

1. Patke, A., Young, M.W., and Axelrod, S. (2020). Molecular mechanisms and physiological importance of circadian rhythms. Nat. Rev. Mol. Cell Biol. *21*, 67–84. https://doi.org/10.1038/s41580-019-0179-2.
2. Hastings, M.H., Maywood, E.S., and Brancaccio, M. (2018). Generation of circadian rhythms in the suprachiasmatic nucleus. Nat. Rev. Neurosci. *19*, 453–469. https://doi.org/10.1038/s41583-018-0026-z.
3. LeGates, T.A., Fernandez, D.C., and Hattar, S. (2014). Light as a central modulator of circadian rhythms, sleep and affect. Nat. Rev. Neurosci. *15*, 443–454. https://doi.org/10.1038/nrn3743.
4. Buhr, E.D., Yoo, S.H., and Takahashi, J.S. (2010). Temperature as a universal resetting cue for mammalian circadian oscillators. Science *330*, 379–385. https://doi.org/10.1126/science.1195262.
5. Stokkan, K.A., Yamazaki, S., Tei, H., Sakaki, Y., and Menaker, M. (2001). Entrainment of the circadian clock in the liver by feeding. Science *291*, 490–493. https://doi.org/10.1126/science.291.5503.490.
6. Wolff, G., and Esser, K.A. (2012). Scheduled exercise phase shifts the circadian clock in skeletal muscle. Med. Sci. Sports Exerc. *44*, 1663–1670. https://doi.org/10.1249/MSS.0b013e318255cf4c.
7. Baron, K.G., and Reid, K.J. (2014). Circadian misalignment and health. Int. Rev. Psychiatry *26*, 139–154. https://doi.org/10.3109/09540261.2014.911149.
8. Stenvers, D.J., Scheer, F.A.J.L., Schrauwen, P., la Fleur, S.E., and Kalsbeek, A. (2019). Circadian clocks and insulin resistance. Nat. Rev. Endocrinol. *15*, 75–89. https://doi.org/10.1038/s41574-018-0122-1.
9. Saini, C., Petrenko, V., Pulimeno, P., Giovannoni, L., Berney, T., Hebrok, M., Howald, C., Dermitzakis, E.T., and Dibner, C. (2016). A functional circadian clock is required for proper insulin secretion by human pancreatic islet cells. Diabetes Obes. Metab. *18*, 355–365. https://doi.org/10.1111/dom.12616.
10. Petrenko, V., Gandasi, N.R., Sage, D., Tengholm, A., Barg, S., and Dibner, C. (2020). In pancreatic islets from type 2 diabetes patients, the dampened circadian oscillators lead to reduced insulin and glucagon exocytosis. Proc. Natl. Acad. Sci. USA *117*, 2484–2495. https://doi.org/10.1073/pnas.1916539117.
11. Mason, I.C., Qian, J., Adler, G.K., and Scheer, F.A.J.L. (2020). Impact of circadian disruption on glucose metabolism: implications for type 2 diabetes. Diabetologia *63*, 462–472. https://doi.org/10.1007/s00125-019-05059-6.
12. Lee, J., Moulik, M., Fang, Z., Saha, P., Zou, F., Xu, Y., Nelson, D.L., Ma, K., Moore, D.D., and Yechoor, V.K. (2013). Bmal1 and beta-cell clock are required for adaptation to circadian disruption, and their loss of function leads to oxidative stress-induced beta-cell failure in mice. Mol. Cell Biol. *33*, 2327–2338. https://doi.org/10.1128/MCB.01421-12.
13. Marcheva, B., Ramsey, K.M., Buhr, E.D., Kobayashi, Y., Su, H., Ko, C.H., Ivanova, G., Omura, C., Mo, S., Vitaterna, M.H., et al. (2010). Disruption of

the clock components CLOCK and BMAL1 leads to hypoinsulinaemia and diabetes. Nature *466*, 627–631. https://doi.org/10.1038/nature09253.

14. Donath, M.Y., Dinarello, C.A., and Mandrup-Poulsen, T. (2019). Targeting innate immune mediators in type 1 and type 2 diabetes. Nat. Rev. Immunol. *19*, 734–746. https://doi.org/10.1038/s41577-019-0213-9.
15. Larsen, C.M., Faulenbach, M., Vaag, A., Vølund, A., Ehses, J.A., Seifert, B., Mandrup-Poulsen, T., and Donath, M.Y. (2007). Interleukin-1-receptor antagonist in type 2 diabetes mellitus. N. Engl. J. Med. *356*, 1517–1526. https://doi.org/10.1056/NEJMoa065213.
16. Quattrin, T., Haller, M.J., Steck, A.K., Felner, E.I., Li, Y., Xia, Y., Leu, J.H., Zoka, R., Hedrick, J.A., Rigby, M.R., et al. (2020). Golimumab and Beta-Cell Function in Youth with New-Onset Type 1 Diabetes. N. Engl. J. Med. *383*, 2007–2017. https://doi.org/10.1056/NEJMoa2006136.
17. Ortis, F., Cardozo, A.K., Crispim, D., Störling, J., Mandrup-Poulsen, T., and Eizirik, D.L. (2006). Cytokine-induced proapoptotic gene expression in insulin-producing cells is related to rapid, sustained, and nonoscillatory nuclear factor-kappaB activation. Mol. Endocrinol. *20*, 1867–1879. https://doi.org/10.1210/me.2005-0268.
18. Berchtold, L.A., Prause, M., Størling, J., and Mandrup-Poulsen, T. (2016). Cytokines and Pancreatic beta-Cell Apoptosis. Adv. Clin. Chem. *75*, 99–158. https://doi.org/10.1016/bs.acc.2016.02.001.
19. Kharroubi, I., Ladrière, L., Cardozo, A.K., Dogusan, Z., Cnop, M., and Eizirik, D.L. (2004). Free fatty acids and cytokines induce pancreatic beta-cell apoptosis by different mechanisms: role of nuclear factor-kappaB and endoplasmic reticulum stress. Endocrinology *145*, 5087–5096. https://doi.org/10.1210/en.2004-0478.
20. Oyadomari, S., Takeda, K., Takiguchi, M., Gotoh, T., Matsumoto, M., Wada, I., Akira, S., Araki, E., and Mori, M. (2001). Nitric oxide-induced apoptosis in pancreatic beta cells is mediated by the endoplasmic reticulum stress pathway. Proc. Natl. Acad. Sci. USA *98*, 10845–10850. https://doi.org/10.1073/pnas.191207498.
21. Meyerovich, K., Ortis, F., Allagnat, F., and Cardozo, A.K. (2016). Endoplasmic reticulum stress and the unfolded protein response in pancreatic islet inflammation. J. Mol. Endocrinol. *57*, R1–R17. https://doi.org/10.1530/jme-15-0306.
22. Hong, H.K., Maury, E., Ramsey, K.M., Perelis, M., Marcheva, B., Omura, C., Kobayashi, Y., Guttridge, D.C., Barish, G.D., and Bass, J. (2018). Requirement for NF-κB in maintenance of molecular and behavioral circadian rhythms in mice. Genes Dev. *32*, 1367–1379. https://doi.org/10.1101/gad.319228.118.
23. Shen, Y., Endale, M., Wang, W., Morris, A.R., Francey, L.J., Harold, R.L., Hammers, D.W., Huo, Z., Partch, C.L., Hogenesch, J.B., et al. (2021). NF-κB modifies the mammalian circadian clock through interaction with the core clock protein BMAL1. PLoS Genet. *17*, e1009933. https://doi.org/10.1371/journal.pgen.1009933.
24. Andersen, P.A.K., Petrenko, V., Rose, P.H., Koomen, M., Fischer, N., Ghiasi, S.M., Dahlby, T., Dibner, C., and Mandrup-Poulsen, T. (2020). Proinflammatory Cytokines Perturb Mouse and Human Pancreatic Islet Circadian Rhythmicity and Induce Uncoordinated β-Cell Clock Gene Expression via Nitric Oxide, Lysine Deacetylases, and Immunoproteasomal Activity. Int. J. Mol. Sci. *22*, 83. https://doi.org/10.3390/ijms22010083.
25. Javeed, N., Brown, M.R., Rakshit, K., Her, T., Sen, S.K., and Matveyenko, A.V. (2021). Pro-inflammatory Cytokine Interleukin 1beta Disrupts beta cell Circadian Clock Function and Regulation of Insulin Secretion. Endocrinology *162*, bqaa084. https://doi.org/10.1210/endocr/bqaa084.
26. Christensen, D.P., Gysemans, C., Lundh, M., Dahllöf, M.S., Noesgaard, D., Schmidt, S.F., Mandrup, S., Birkbak, N., Workman, C.T., Piemonti, L., et al. (2014). Lysine deacetylase inhibition prevents diabetes by chromatin-independent immunoregulation and beta-cell protection. Proc. Natl. Acad. Sci. USA *111*, 1055–1059. https://doi.org/10.1073/pnas.1320850111.
27. Balsalobre, A., Damiola, F., and Schibler, U. (1998). A serum shock induces circadian gene expression in mammalian tissue culture cells. Cell *93*, 929–937. https://doi.org/10.1016/s0092-8674(00)81199-x.
28. Yagita, K., and Okamura, H. (2000). Forskolin induces circadian gene expression of rPer1, rPer2 and dbp in mammalian rat-1 fibroblasts. FEBS Lett. *465*, 79–82. https://doi.org/10.1016/s0014-5793(99)01724-x.
29. Perelis, M., Marcheva, B., Ramsey, K.M., Schipma, M.J., Hutchison, A.L., Taguchi, A., Peek, C.B., Hong, H., Huang, W., Omura, C., et al. (2015). Pancreatic beta cell enhancers regulate rhythmic transcription of genes controlling insulin secretion. Science *350*, aac4250. https://doi.org/10.1126/science.aac4250.
30. Petrenko, V., Saini, C., Giovannoni, L., Gobet, C., Sage, D., Unser, M., Heddad Masson, M., Gu, G., Bosco, D., Gachon, F., et al. (2017). Pancreatic alpha- and beta-cellular clocks have distinct molecular properties and impact on islet hormone secretion and gene expression. Genes Dev. *31*, 383–398. https://doi.org/10.1101/gad.290379.116.
31. Stratmann, M., Suter, D.M., Molina, N., Naef, F., and Schibler, U. (2012). Circadian Dbp transcription relies on highly dynamic BMAL1-CLOCK interaction with E boxes and requires the proteasome. Mol. Cell *48*, 277–287. https://doi.org/10.1016/j.molcel.2012.08.012.
32. Broniowska, K.A., Oleson, B.J., and Corbett, J.A. (2014). beta-Cell responses to nitric oxide. Vitam. Horm. *95*, 299–322. https://doi.org/10.1016/B978-0-12-800174-5.00012-0.
33. Ziegelbauer, K., Gantner, F., Lukacs, N.W., Berlin, A., Fuchikami, K., Niki, T., Sakai, K., Inbe, H., Takeshita, K., Ishimori, M., et al. (2005). A selective novel low-molecular-weight inhibitor of IkappaB kinase-beta (IKK-beta) prevents pulmonary inflammation and shows broad anti-inflammatory activity. Br. J. Pharmacol. *145*, 178–192. https://doi.org/10.1038/sj.bjp.0706176.
34. Hansen, J.B., Tonnesen, M.F., Madsen, A.N., Hagedorn, P.H., Friberg, J., Grunnet, L.G., Heller, R.S., Nielsen, A.Ø., Størling, J., Baeyens, L., et al. (2012). Divalent metal transporter 1 regulates iron-mediated ROS and pancreatic beta cell fate in response to cytokines. Cell Metab. *16*, 449–461. https://doi.org/10.1016/j.cmet.2012.09.001.
35. Benazra, M., Lecomte, M.J., Colace, C., Müller, A., Machado, C., Pechberty, S., Bricout-Neveu, E., Grenier-Godard, M., Solimena, M., Scharfmann, R., et al. (2015). A human beta cell line with drug inducible excision of immortalizing transgenes. Mol. Metab. *4*, 916–925. https://doi.org/10.1016/j.molmet.2015.09.008.
36. Spinas, G.A., Mandrup-Poulsen, T., Mølvig, J., Baek, L., Bendtzen, K., Dinarello, C.A., and Nerup, J. (1986). Low concentrations of interleukin-1 stimulate and high concentrations inhibit insulin release from isolated rat islets of Langerhans. Acta Endocrinol. *113*, 551–558. https://doi.org/10.1530/acta.0.1130551.
37. Mandrup-Poulsen, T., Bendtzen, K., Nerup, J., Dinarello, C.A., Svenson, M., and Nielsen, J.H. (1986). Affinity-purified human interleukin I is cytotoxic to isolated islets of Langerhans. Diabetologia *29*, 63–67. https://doi.org/10.1007/bf02427283.
38. Zambrano, S., De Toma, I., Piffer, A., Bianchi, M.E., and Agresti, A. (2016). NF-κB oscillations translate into functionally related patterns of gene expression. Elife *5*, e09100. https://doi.org/10.7554/eLife.09100.
39. Chaisson, M.L., Brooling, J.T., Ladiges, W., Tsai, S., and Fausto, N. (2002). Hepatocyte-specific inhibition of NF-kappaB leads to apoptosis after TNF treatment, but not after partial hepatectomy. J. Clin. Investig. *110*, 193–202. https://doi.org/10.1172/jci15295.
40. Mandrup-Poulsen, T., Pickersgill, L., and Donath, M.Y. (2010). Blockade of interleukin 1 in type 1 diabetes mellitus. Nat. Rev. Endocrinol. *6*, 158–166. https://doi.org/10.1038/nrendo.2009.271.
41. Cannon, J.G., Tompkins, R.G., Gelfand, J.A., Michie, H.R., Stanford, G.G., van der Meer, J.W., Endres, S., Lonnemann, G., Corsetti, J., Chernow, B., et al. (1990). Circulating interleukin-1 and tumor necrosis factor in septic shock and experimental endotoxin fever. J. Infect. Dis. *161*, 79–84. https://doi.org/10.1093/infdis/161.1.79.
42. McNulty, A.L., Rothfusz, N.E., Leddy, H.A., and Guilak, F. (2013). Synovial fluid concentrations and relative potency of interleukin-1 alpha and beta in cartilage and meniscus degradation. J. Orthop. Res. *31*, 1039–1045. https://doi.org/10.1002/jor.22334.

43. Malyak, M., Swaney, R.E., and Arend, W.P. (1993). Levels of synovial fluid interleukin-1 receptor antagonist in rheumatoid arthritis and other arthropathies. Potential contribution from synovial fluid neutrophils. Arthritis Rheum. *36*, 781–789. https://doi.org/10.1002/art.1780360607.

44. Ferrington, D.A., and Gregerson, D.S. (2012). Immunoproteasomes: structure, function, and antigen presentation. Prog. Mol. Biol. Transl. Sci. *109*, 75–112. https://doi.org/10.1016/b978-0-12-397863-9.00003-1.

45. Khilji, M.S., Verstappen, D., Dahlby, T., Burstein Prause, M.C., Pihl, C., Bresson, S.E., Bryde, T.H., Keller Andersen, P.A., Klindt, K., Zivkovic, D., et al. (2020). The intermediate proteasome is constitutively expressed in pancreatic beta cells and upregulated by stimulatory, low concentrations of interleukin 1 β. PLoS One *15*, e0222432. https://doi.org/10.1371/journal.pone.0222432.

46. Brown, M.R., Laouteouet, D., Delobel, M., Villard, O., Broca, C., Bertrand, G., Wojtusciszyn, A., Dalle, S., Ravier, M.A., Matveyenko, A.V., and Costes, S. (2022). The nuclear receptor REV-ERBα is implicated in the alteration of β-cell autophagy and survival under diabetogenic conditions. Cell Death Dis. *13*, 353. https://doi.org/10.1038/s41419-022-04767-z.

47. Jung, H.S., Chung, K.W., Won Kim, J., Kim, J., Komatsu, M., Tanaka, K., Nguyen, Y.H., Kang, T.M., Yoon, K.H., Kim, J.W., et al. (2008). Loss of autophagy diminishes pancreatic beta cell mass and function with resultant hyperglycemia. Cell Metab. *8*, 318–324. https://doi.org/10.1016/j.cmet.2008.08.013.

48. Sulli, G., Rommel, A., Wang, X., Kolar, M.J., Puca, F., Saghatelian, A., Plikus, M.V., Verma, I.M., and Panda, S. (2018). Pharmacological activation of REV-ERBs is lethal in cancer and oncogene-induced senescence. Nature *553*, 351–355. https://doi.org/10.1038/nature25170.

49. Barber, R., and Butcher, R.W. (1980). The turnover of cyclic AMP in cultured fibroblasts. J. Cyclic Nucleotide Res. *6*, 3–14.

50. Mourad, N.I., Nenquin, M., and Henquin, J.C. (2012). cAMP-mediated and metabolic amplification of insulin secretion are distinct pathways sharing independence of β-cell microfilaments. Endocrinology *153*, 4644–4654. https://doi.org/10.1210/en.2012-1450.

51. Jhala, U.S., Canettieri, G., Screaton, R.A., Kulkarni, R.N., Krajewski, S., Reed, J., Walker, J., Lin, X., White, M., and Montminy, M. (2003). cAMP promotes pancreatic beta-cell survival via CREB-mediated induction of IRS2. Genes Dev. *17*, 1575–1580. https://doi.org/10.1101/gad.1097103.

52. Gerlo, S., Kooijman, R., Beck, I.M., Kolmus, K., Spooren, A., and Haegeman, G. (2011). Cyclic AMP: a selective modulator of NF-κB action. Cell. Mol. Life Sci. *68*, 3823–3841. https://doi.org/10.1007/s00018-011-0757-8.

53. Pipeleers, D.G., Schuit, F.C., in't Veld, P.A., Maes, E., Hooghe-Peters, E. L., Van de Winkel, M., and Gepts, W. (1985). Interplay of nutrients and hormones in the regulation of insulin release. Endocrinology *117*, 824–833. https://doi.org/10.1210/endo-117-3-824.

54. Liu, D., Pavlovic, D., Chen, M.C., Flodström, M., Sandler, S., and Eizirik, D. L. (2000). Cytokines induce apoptosis in beta-cells isolated from mice lacking the inducible isoform of nitric oxide synthase (iNOS-/-). Diabetes *49*, 1116–1122. https://doi.org/10.2337/diabetes.49.7.1116.

55. Corbett, J.A., Sweetland, M.A., Wang, J.L., Lancaster, J.R., Jr., and McDaniel, M.L. (1993). Nitric oxide mediates cytokine-induced inhibition of insulin secretion by human islets of Langerhans. Proc. Natl. Acad. Sci. USA *90*, 1731–1735. https://doi.org/10.1073/pnas.90.5.1731.

56. Eizirik, D.L., Sandler, S., Welsh, N., Cetkovic-Cvrlje, M., Nieman, A., Geller, D.A., Pipeleers, D.G., Bendtzen, K., and Hellerström, C. (1994). Cytokines suppress human islet function irrespective of their effects on nitric oxide generation. J. Clin. Investig. *93*, 1968–1974. https://doi.org/10.1172/jci117188.

57. Cardozo, A.K., Heimberg, H., Heremans, Y., Leeman, R., Kutlu, B., Kruhøffer, M., Ørntoft, T., and Eizirik, D.L. (2001). A comprehensive analysis of cytokine-induced and nuclear factor-kappa B-dependent genes in primary rat pancreatic beta-cells. J. Biol. Chem. *276*, 48879–48886. https://doi.org/10.1074/jbc.M108658200.

58. Cardozo, A.K., Kruhøffer, M., Leeman, R., Orntoft, T., and Eizirik, D.L. (2001). Identification of novel cytokine-induced genes in pancreatic beta-cells by high-density oligonucleotide arrays. Diabetes *50*, 909–920. https://doi.org/10.2337/diabetes.50.5.909.

59. Zieliński, T., Hay, J., and Millar, A.J. (2022). Period Estimation and Rhythm Detection in Timeseries Data Using BioDare2, the Free, Online, Community Resource. Methods Mol. Biol. *2398*, 15–32. https://doi.org/10.1007/978-1-0716-1912-4_2.

60. Gomez-Perosanz, M., Ras-Carmona, A., and Reche, P.A. (2020). PCPS: A Web Server to Predict Proteasomal Cleavage Sites. Methods Mol. Biol. *2131*, 399–406. https://doi.org/10.1007/978-1-0716-0389-5_23.

61. Yoo, S.H., Yamazaki, S., Lowrey, P.L., Shimomura, K., Ko, C.H., Buhr, E. D., Siepka, S.M., Hong, H.K., Oh, W.J., Yoo, O.J., et al. (2004). PERIOD2::LUCIFERASE real-time reporting of circadian dynamics reveals persistent circadian oscillations in mouse peripheral tissues. Proc. Natl. Acad. Sci. USA *101*, 5339–5346. https://doi.org/10.1073/pnas.0308709101.

62. Parnaud, G., Hammar, E., Ribaux, P., Donath, M.Y., Berney, T., and Halban, P.A. (2009). Signaling pathways implicated in the stimulation of beta-cell proliferation by extracellular matrix. Mol. Endocrinol. *23*, 1264–1271. https://doi.org/10.1210/me.2009-0008.

STAR★METHODS

KEY RESOURCES TABLE

REAGENT or RESOURCE	SOURCE	IDENTIFIER
Antibodies		
See Table S4	N/A	N/A
Chemicals, peptides, and recombinant proteins		
Blasticidin S	Thermo Fischer Scientific (Gibco™)	Cat# R21001
BSA without fatty acid	Gerbu Biotechnik	Cat# 1066
Collagenase Type XI	Sigma-Aldrich	Cat# C7657
cOmplete™, Mini, EDTA-free Protease Inhibitor Cocktail	Sigma-Aldrich	Cat# 11836170001
DMEM, low glucose, pyruvate	Thermo Fischer Scientific (Gibco™)	Cat# 11885084
Firefly D-Luciferin Free Acid	NanoLight Technology	Cat# 306-FA
Forskolin	Sigma-Aldrich	Cat# 344270
Gentamicin	Thermo Fischer Scientific (Gibco™)	Cat# 11360-070
Gentamicin	Thermo Fischer Scientific (Gibco™)	Cat# 15710-049
Heat-inactivated Fetal Bovine Serum	Thermo Fischer Scientific (Gibco™)	Cat# 10500064
HEPES	Thermo Fischer Scientific (Gibco™)	Cat# 15630-056
Human Transferrin	Sigma-Aldrich	Cat# T8158
Liberase	Roche	Cat# 05401020001
Nicotinamide	Sigma-Aldrich	Cat# N0636
Penicillin-Streptomycin	Thermo Fischer Scientific (Gibco™)	Cat# 15140122
Recombinant Mouse IL-1β	R&D Systems	Cat# 401-ML-005
Recombinant Rat IFN-γ	R&D Systems	Cat# 585-IF-100
RPMI 1640 Medium, GlutaMAX™ Supplement	Thermo Fischer Scientific (Gibco™)	Cat# 61870036
RPMI 1640 Medium, GlutaMAX™ Supplement No phenol red	Thermo Fischer Scientific (Gibco™)	Cat# 11835
Sodium Pyruvate	Thermo Fischer Scientific (Gibco™)	Cat# 11360-070
Sodium selenite	Thermo Scientific Chemicals	Cat# 012585-22
VivoGlo™ Luciferin	Promega	Cat# P1041
Critical commercial assays		
AlamarBlue™ HS Cell Viability Reagent	Thermo Fisher Scientific (Invitrogen™)	Cat# A50100
Caspase-Glo™ 3/7 Assay System	Promega	Cat# G8090
Caspase-Glo™ 8 Assay System	Promega	Cat# G8200
Caspase-Glo™ 9 Assay System	Promega	Cat# G8210
CellTox™ Green Cytotoxicity Assay	Promega	Cat# G8741
iScript™ cDNA Synthesis Kit	Bio-Rad Laboratories	Cat# 1708891
NucleoSpin® RNA	Macherey-Nagel	Cat# 740984
SYBR™ Green Universal Master Mix	Thermo Fisher Scientific (Applied Biosystems ™)	Cat# 4309155
TotalStain Q –PVDF Fluorescent Total Protein Staining Kit	Azure Biosystems	Cat# AC2225
Experimental models: Cell lines		
Human: EndoC-βH3	Human Cell Design	RRID: CVCL_IS72
Human: HEK293T	N/A	RRID: CVCL_0063

(*Continued on next page*)

Continued

REAGENT or RESOURCE	SOURCE	IDENTIFIER
Rat: INS-1	Gift from C. Wollheim and P. Maechler, University Medical Centre, Geneva, Switzerland	RRID: CVCL_0352
Experimental models: Organisms/strains		
Mouse: C57Bl/6J	Charles River Laboratories	RRID: IMSR_CRL:027
Mouse: C57BL/6J mPer2:Luc	The Jackson Laboratory	RRID: IMSR_JAX:006852
Oligonucleotides		
For primers see Table S3	TAG Copenhagen	N/A
Recombinant DNA		
pPer2:Luc	Gift from Prof. Louis Ptáček, University of California San Francisco	N/A
psPAX2	N/A	RRID: Addgene_12260
pMD2.G	N/A	RRID: Addgene_12259
Software and algorithms		
AzureSpot Pro	Azure Biosystems	https://azurebiosystems.com/software/azurespotpro/
BioDare2	Zieliński et al.[59]	https://biodare2.ed.ac.uk/
GraphPad Prism 9/10	GraphPad Software	https://www.graphpad.com/
Image Lab 6.1	Bio-Rad Laboratories	https://www.bio-rad.com/product/image-lab-software?ID=KRE6P5E8Z
Improved Proteasome Cleavage Prediction Server (iPCPS)	Gomez-Perosanz et al.[60]	http://imed.med.ucm.es/Tools/pcps/
QuantStudio™ Design & Analysis Software	Applied Biosystems	https://www.thermofisher.com/home/technical-resources/software-downloads/quantstudio-3-5-real-time-pcr-systems.html
Other		
Azure®Saphire Biomolecular Imager	Azure Biosystems	N/A
CLARIOstar Plus with Atmospheric Control Unit (ACU)	BMG LABTECH	N/A
Histopaque®-1077 Hybri-Max™	Sigma-Aldrich	Cat# H8889
Histopaque®-1119	Sigma-Aldrich	Cat# 11191
iBLOT2 system	Thermo Fisher Scientific (Invitrogen™)	N/A
iBlot™ 2 Transfer Stacks, PVDF, mini	Thermo Fisher Scientific (Invitrogen™)	Cat# IB24002
LumiCycle	Actimetrics	N/A
NuPAGE™ Bis-Tris Mini Protein Gels, 4–12%, 1.0–1.5 mm	Thermo Fisher Scientific (Invitrogen™)	Cat# NP0323BOX
QuantStudio5™	Applied Biosystems	N/A
Radiance Q Chemiluminescent Substrate	Azure Biosystems	Cat# AC2101
SpectraMax® i3x	Molecular Devices	N/A

EXPERIMENTAL MODEL AND STUDY PARTICIPANT DETAILS

Mice

Murine pancreatic islets used for qPCR and cytotoxicity assays were isolated from 11-12 -week-old C57Bl/6J female mice weighing 21.7±0.25 g (range 20.2-23.9 g) (Charles River Laboratories Germany). The mice were housed in a temperature-controlled environment with a 12h:12h light-dark cycle and *ad libitum* access to chow (Altromin 1310, Lage, Germany) and water. All procedures were approved by local veterinarians (project number P24-378) and carried out in accordance with Danish guidelines and regulations and the EU directive 2010/63/EU for the protection of animals used for scientific purposes. Mice were housed for at least two weeks at the facility for acclimatization before experimentation.

Pancreatic islets for circadian bioluminescence recordings were isolated from adult (approximately 15 weeks old) female C57BL/6J mice expressing the circadian reporter Per2-luciferase (*mPer2:Luc*) (The Jackson Laboratory, Bar Harbor, ME, USA).[61] Mice were kept under standard temperature-controlled animal housing conditions with *ad libitum* access to food and water and 12h:12h light-dark cycle. All animal experiments were conducted in compliance with the guidelines of the Canton of Geneva, Switzerland.

Cell culture

The rat INS-1 insulinoma cell line (from male rat origin) was kindly provided by C. Wollheim and P. Maechler, University Medical Centre, Geneva, Switzerland. Cells were cultured in RPMI-1640 with GlutaMAX™, and supplemented with 10% FBS, 1% penicillin/streptomycin, HEPES, sodium bicarbonate, and 50 μM β-mercaptoethanol (culture medium) (Gibco, Thermo Fisher Scientific, Waltham, Massachusetts, USA). The EndoC-βH3 cell line (sex unspecified) was purchased from Human Cell Design (Toulouse, France) and cultured in low glucose DMEM (Gibco, Thermo Fisher Scientific) supplemented with 50 μM β-mercaptoethanol, 1% penicillin/streptomycin (Gibco, Thermo Fisher Scientific), 2% BSA (Gerbu Biotechnik, Heidelberg, Germany), 6.7 ng/mL sodium selenite (Thermo Fisher Chemicals), 10 mM Nicotinamide, and 5.5 μg/mL Human Transferrin (Sigma-Aldrich). The cells were exposed to proinflammatory cytokines, inhibitors, and conditions in the concentrations and for the time periods specified in figure legends. Concentrations of cytokines were chosen from dose-response curves for the effect of IL-1β on clock gene expression and rhythmic parameters, as published by us[24] (Figures 1 and 2). The addition of IFN-γ did not qualitatively alter the effects of IL-1β alone[24] (Figure 3), which is why we decided not to test IFN-γ alone in this study. For functional assays using absorbance, luminescence, or fluorescence, culture medium without phenol red was used.

Pancreatic islet isolation

Pancreatic islets for qPCR and cytotoxicity assays were isolated by injecting liberase (Roche, Basel, Switzerland; 0.1 mg/mL dissolved in HBSS) into the common bile duct immediately after euthanasia, after which the pancreas was immersed in a water bath at 37°C and shaken. The resulting digest was placed on ice and three-four washing rounds were conducted by collecting the supernatant after 5 min of incubation on ice and replacing the salt solution. The islets were then handpicked under a stereo microscope (Leica, Heerbrugg, Switzerland) and transferred twice to fresh dishes containing RPMI 1640+glutamax (11 mM glucose) supplemented with 10% fetal bovine serum and 1% penicillin/streptomycin (Gibco, Thermo Fisher Scientific). The isolated islets were incubated at 37°C and 5% CO_2 for at least 48 hours before experimentation, with a medium change the day after isolation. On day 2, 180 islets per condition (from an islet pool isolated from 4-5 mice) were transferred into six dishes per biological replicate. Four individual biological replicates were assessed. On day 4, islets were exposed to the experimental conditions, as described in RT-qPCR and Cytotoxicity.

mPer2:Luc islets were obtained using a standard protocol involving collagenase digestion (Type XI, Sigma-Aldrich Sigma-Aldrich, St. Louis, Missouri, USA) of the pancreas, followed by purification on a gradient of Histopaque®-1077 Hybri-Max™ (Sigma-Aldrich) and Histopaque®-1119 (Sigma-Aldrich). After isolation, approximately 250 islets per condition were cultured in multi-well plates precoated with a laminin-5-rich extracellular matrix.[62] Islets were cultured in RPMI Medium 1640 with GlutaMAX supplemented with 10% FBS (Gibco, Thermo Fisher Scientific), 1% penicillin-streptomycin mix (Sigma-Aldrich), 50 μg/mL Gentamicin (10 mg/mL), 10 μM Sodium Pyruvate (100 mM), and 10 mM HEPES buffer solution (1 M)(Gibco, Thermo Fisher Scientific). The isolated islets were incubated at 37°C and 5% CO_2 for 48 hours before experimentation.

METHOD DETAILS

RT-qPCR

One-hundred forty islets per dish were transferred into a 60 mm dish for 12-hour long exposure, while $0.5x10^6$ INS-1 cells/well were seeded in a 6 well-plate for three days before exposure. RNA was extracted using NucleoSpin® RNA kit (Macherey-Nagel, Bethlehem, PA, USA). RNA quality and quantity were assessed using Nanodrop-2000 (Thermo Fisher Scientific, Waltham, MA, USA). cDNA was synthesized from 500 ng RNA using the iScript™-cDNA Kit (Bio-Rad Laboratories, Hercules, CA, USA). Real-time quantitative PCR was carried out using mRNA-specific primers (Table S3), designed in-lab and synthesized by TAG Copenhagen (Copenhagen, Denmark), and SYBR™ Green PCR Master Mix (Applied Biosystems, Waltham, MA, USA). Amplification and real-time monitoring were carried out using QuantStudio5, and data was analyzed using QuantStudio™ Design & Analysis Software (Applied Biosystems). All reactions were carried out following the manufacturer's protocols. mRNA expression was visualized as normalized expression using the $2^{-\Delta\Delta Ct}$ method (ΔCt (exposed sample) – ΔCt (control sample), where ΔCt values are defined as $Ct_{target\ gene}$-$Ct_{reference\ gene}$. Statistical differences in relative mRNA expression were determined using log2 transformed data, as the normalized expression was not normally distributed. Thus, when depicted graphically as non-transformed data, SEMs may overlap yet still be statistically different. The stability of multiple reference mRNAs was evaluated based on raw Ct values, using the most stable mRNAs for normalization in the given experimental setup as given in the figure legends. If two or more reference genes provided the least variation in Ct values, the geometric mean of the genes was used.

Western blotting

Cells were lysed in lysis buffer consisting of 100 mM Tris (pH 8.0), 30 mM NaCl, 10 mM KCl, 10 mM MgCl2, 2% IGEPAL, 20 mM iodoacetamide and Roche Protease inhibitor tablets (Sigma-Aldrich). Protein concentrations were measured by Bradford assay using Bio-Rad Protein Assay Dye Reagent (Bio-Rad Laboratories). Indicated amounts of protein were loaded on Nu-Page 4-12% bis-tris gels (Thermo Fisher Scientific), separated by SDS-PAGE, and transferred to PVDF membranes via the iBLOT2 system (Thermo Fisher Scientific). Total protein on the blots was detected using TotalStain Q – PVDF Fluorescent Total Protein Staining Kit (Azure Biosystems, Ohio, USA), and captured using the Azure®Saphire Biomolecular Imager (Azure Biosystems). Membranes were blocked using 5% skim-milk powder (MilliporeSigma, Massachusetts, USA) for one hour, following incubation with primary antibodies (Table S4) diluted in TBST, containing 2% BSA and 0.27% sodium azide or in azure blocking buffer with sodium azide, overnight. Membranes were incubated with the appropriate secondary antibodies (dilution 1:10,000) for two hours. The final blots were developed by means of chemiluminescence using Radiance Q Chemiluminescent Substrate (Azure Biosystems). Image Lab 6.1 (Bio-Rad Laboratories) and AzureSpot Pro (Azure Biosystems) were used for densitometric analysis of the Western Blots. Antibodies and dilutions are annotated in Table S4. Expression levels for the proteins of interest were quantified as relative expression to GAPDH as reference protein. GAPDH was selected based on low within blot variance between conditions. Additionally, minimal variance in protein loading was confirmed by total protein staining. Quantified values are normalized using a built-in normalization method in GraphPad Prism 10 (GraphPad Software, Boston, MA, USA), in which 0 is set as 0%, while 100% is determined as the mean of the signal from biological replicates within an experimental condition of either 8 or 36 hours, depending on which value was the greater. In the process of finding suitable antibodies, five different PER2 antibodies from various sources were tested. However, none of these provided quantifiable signals, thus limiting the number of clock specific antibodies to BMAL1, CLOCK, REV-ERBα and CRY2.

Lentiviral transduction of INS-1 cells

Lentiviral particles were produced by transfecting 293T cells in 10 cm dishes with helper plasmids Pax2 and MD.2g together with either Period 2 promotor-driven Luciferase (*Per2:Luc*) (a gift from Prof. Louis Ptáček, University of California, San Francisco, US) or GFP lentivectors by calcium phosphate transfection. Virus supernatant was collected after 48 hours and concentrated 20X in Amicon filters with a 100,000 kDa cut-off. INS-1 cells were transduced with either *Per2:Luc* or GFP lentiviral particles over 48 hours, and approximate transduction efficiency was assessed by GFP transduction in parallel cultures. *Per2:Luc* transduced cells corresponding to a GFP expression of ∼65% (one virus integration per genome) were selected with blasticidin.

In vitro synchronization

Murine islets, INS-1 and EndoC-βH3 cells were synchronized using a one-hour 10 μM forskolin pulse (Sigma-Aldrich), followed by washing with 37°C warm medium, and incubation in medium with the exposures, as described in.[24,28] When cells or islets were exposed to experimental conditions such as cytokines, while also subjected to *in vitro* synchronization, cells were co-incubated with the experimental condition (e.g. cytokines) and forskolin in the one-hour pulse. At the end of the pulse, cells were washed, and then the experimental exposures were added for the remaining duration of the experiment.

Circadian bioluminescence recording

Continuous bioluminescence from synchronized islets was recorded for four days in 10-minute intervals, in media containing 0.1 mM D-luciferin (Firefly Luciferin Free Acid, NanoLight Technology, Pinetop, AZ, USA). The parafilm-sealed plates were placed for recording in a LumiCycle (Actimetrics, Wilmette, IL, USA) at 37°C and 5% CO_2. The amplitude, period length, and circadian phase of the raw bioluminescence signals were determined from detrended data, represented as a moving average with a 24-hour window.[30] Circadian parameters were estimated by the mFourFit method carried out using BioDare2[59] starting 24 hours after the initiation of recording. Data were generated from islets obtained from two independent isolations using pools of 7-12 female mice.

INS-1 *Per2:Luc* cells were incubated for 24 hours in a white-walled and -bottomed 96-well plate (15,000 cells/well). After exposures and forskolin pulse, the cells were incubated in culture medium without phenol red with 0.1 mM D-luciferin (VivoGlo™ Luciferin, Promega, Madison, WI, USA) (experimental medium). Bioluminescence was recorded using the CLARIOstar Plus, with an atmospheric control unit (ACU) (BMG LABTECH, Ortenberg, Germany) to allow for continuous 96-hour monitoring at 10-minute intervals at 37°C and 5% CO_2. Raw traces were detrended using a 24-hour window moving average. The functional window defined below was used to determine rhythmic parameters by the mFourFit method carried out using BioDare2.[59] At low concentrations of IL-1β (≤15 pg/mL), the functional window was set from 13.5 to 85.5 hours of the recording. At high IL-1β (≥30 pg/mL), the functional window was set from 30 to 85.5 hours of the recording, due to the noisy initial 30-hour period preventing rhythmic analysis, as illustrated in the detrended bioluminescence recordings.

Viability

INS-1 cells were seeded at 30,000 cells per well in a clear 96-well plate for 3 days, followed by exposures as described in the figure legends. Mitochondrial function was determined using AlamarBlue™ HS Cell Viability Reagent (Invitrogen, Waltham, MA, USA) as a proxy for cell viability, following the manufacturer's protocol, and absorbance or fluorescence recorded on a SpectraMax® i3x (Molecular Devices, San Jose, CA, USA).

Cytotoxicity

Total accumulated cytotoxicity (an integrated readout for apoptosis and late apoptotic necrosis) was monitored in real-time using the Cell-tox assay (Promega) according to the manufacturer's protocol. Twenty murine islets per well were transferred to a 96-well black-walled plate, while INS-1 cells were seeded in either a black-walled plate, if the toxicity assay was run alone, or in a white-walled plate if multiplexed with the circadian bioluminescence assay. Murine islets and INS-1 cells were incubated in non-phenol red complete RPMI medium and monitored in real-time at 10-minute intervals for five days (murine islets) or 72-96 hours (INS-1) using the CLARIOstar Plus, with ACU (BMG LABTECH) at 37°C and 5% CO_2.

Murine reporter islets were examined morphologically at baseline and the end of bioluminescence monitoring and photomicrographs were taken. There were no systematic differences in islet morphology between conditions at the end of the monitoring period.

Caspase assay

Caspase activity was measured following the manufacturer's instructions using the Caspase-Glo™ 3/7, 8, and 9 Assays (Promega). Ten thousand cells per well were seeded in a white-walled 96-well plate for 48 hours, followed by exposures for 24 hours. Luminescence was measured using a SpectraMax® i3x (Molecular Devices) after a 30-minute incubation with the assay reagents.

Bioinformatics

Proteasomal and immunoproteasomal cleavage sites of selected clock proteins were predicted using the ''Improved Proteasome Cleavage Prediction Server'' (iPCPS) (http://imed.med.ucm.es/Tools/pcps/).[60]

QUANTIFICATION AND STATISTICAL ANALYSIS

Data were analyzed using GraphPad Prism 9/10 as specified in the figure legends. Data are presented as means ± SEMs. Significance levels are annotated as follows: ns = not significant, * = p-value < 0.05, ** = p-value < 0.01, *** = p-value < 0.001, **** = p-value < 0.0001.